© 2014. Published by The Company of Biologists Ltd | Development (2014) 141, 3277-3288 doi:10.1242/dev.110528

RESEARCH ARTICLE

TECHNIQUES AND RESOURCES

# Visualization of the *Drosophila* dKeap1-CncC interaction on chromatin illumines cooperative, xenobiotic-specific gene activation

**Huai Deng and Tom K. Kerppola***

## ABSTRACT

Interactions among transcription factors control their physiological functions by regulating their binding specificities and transcriptional activities. We implement a strategy to visualize directly the genomic loci that are bound by multi-protein complexes in single cells in *Drosophila*. This method is based on bimolecular fluorescence complementation (BiFC) analysis of protein interactions on polytene chromosomes. *Drosophila* Keap1 (dKeap1)-CncC complexes localized to the nucleus and bound chromatin loci that were not bound preferentially by dKeap1 or CncC when they were expressed separately. dKeap1 and CncC binding at these loci was enhanced by phenobarbital, but not by *tert*-butylhydroquinone (tBHQ) or paraquat. Endogenous dKeap1 and CncC activated transcription of the *Jheh* (*Jheh1, Jheh2, Jheh3*) and *dKeap1* genes at these loci, whereas CncC alone activated other xenobiotic response genes. Ectopic dKeap1 expression increased CncC binding at the *Jheh* and *dKeap1* gene loci and activated their transcription, whereas dKeap1 inhibited CncC binding at other xenobiotic response gene loci and suppressed their transcription. The combinatorial chromatin-binding specificities and transcriptional activities of dKeap1-CncC complexes mediated the selective activation of different sets of genes by different xenobiotic compounds, in part through feed-forward activation of *dKeap1* transcription.

**KEY WORDS: Imaging, Bimolecular fluorescence complementation (BiFC), DNA-binding specificity, Combinatorial regulation, Transcription complex, Transcriptional response, *Drosophila* polytene chromosome, Chromatin, Xenobiotic compounds**

## INTRODUCTION

The combinatorial regulation of transcription is essential for the selectivity of eukaryotic gene expression. Chromatin immunoprecipitation studies have revealed that many transcription factors bind overlapping genomic regions (Negre et al., 2011; ENCODE Project Consortium, 2012). In tissues and in heterogeneous cell populations it is difficult to determine whether proteins that bind to the same region contact each other or whether they bind independently to adjacent recognition sequences in different cells.

Bimolecular fluorescence complementation (BiFC) analysis enables the visualization of protein interactions in living cells and tissues (Hu et al., 2002; Plaza et al., 2008; Gohl et al., 2010; Bai and Kerppola, 2011; Hudry et al., 2011; Papadopoulos et al., 2012; Boube et al., 2014). In the BiFC assay, the interaction between two proteins is detected based on the fluorescence produced by the association of two fragments of a fluorescent protein that are fused to two interaction partners. BiFC analysis has also been used to image interactions between epigenetic regulatory proteins and chromatin (Vincenz and Kerppola, 2008). However, it has not been possible to determine the genes that are bound by multi-protein complexes using BiFC analysis because of the difficulty of mapping the genomic loci that are bound by BiFC complexes in diploid cells. To overcome this limitation, we adapted BiFC analysis to study multi-protein complex binding on *Drosophila* polytene chromosomes.

Transcriptional responses to synthetic chemicals (xenobiotic compounds) are regulated by xenobiotic response regulators (Jennings et al., 2013). Cap-n-collar isoform C (CncC) and Nrf2 (also known as Nfe2l2) are homologous *Drosophila* and mammalian bZIP family transcription factors that can bind to and activate genes that express proteins that can protect cells from the deleterious effects of many xenobiotic compounds (Moi et al., 1994; Venugopal and Jaiswal, 1996; McGinnis et al., 1998; Sykiotis and Bohmann, 2008; Malhotra et al., 2010; Misra et al., 2011). Nrf2-deficient mice are more sensitive to chemical carcinogens than wild-type mice, presumably owing to the loss of cytoprotective functions of Nrf2 (Slocum and Kensler, 2011). Depletion of CncC in adult flies reduces the activation of many genes by xenobiotic compounds (Misra et al., 2011). *Drosophila* Keap1 (dKeap1) and mammalian Keap1 are homologous Kelch family proteins that can inhibit the activation of some xenobiotic response genes by CncC and Nrf2, respectively (Itoh et al., 1999; Wakabayashi et al., 2003; Sykiotis and Bohmann, 2008; Misra et al., 2011). Keap1-Nrf2 interaction is essential for Keap1 inhibition of transcriptional activation by Nrf2 (Itoh et al., 1999; McMahon et al., 2006). Depletion of dKeap1 in adult flies increases the transcription of some xenobiotic response genes that are activated by CncC (Misra et al., 2011). The conservation of many dKeap1-CncC and Keap1-Nrf2 functions between insects and mammals (Sykiotis and Bohmann, 2008; Misra et al., 2011) suggested that their interactions might also have conserved effects on their functions.

Both dKeap1 and CncC in *Drosophila* and Keap1 and Nrf2 in mouse also regulate development. *Keap1* deletion in mouse causes hyperkeratosis in the esophagus and forestomach, and *Nrf2* deletion causes defects in adipogenesis and in hematopoiesis (Wakabayashi et al., 2003; Pi et al., 2010; Tsai et al., 2013). Loss-of-function mutations in *dKeap1* and in *cncC* cause larval lethality (Veraksa et al., 2000; Sykiotis and Bohmann, 2008). dKeap1 and CncC regulate *Drosophila* pupation and metamorphosis by binding to and activating ecdysone biosynthesis genes and ecdysone response genes in different tissues (Deng and Kerppola, 2013). The progression of metamorphosis, which is promoted by ecdysone, can be counteracted by juvenile hormone (Dubrovsky, 2005; Riddiford et al., 2010). Juvenile hormone

Department of Biological Chemistry, University of Michigan, Ann Arbor, MI 48109-0650, USA.

*Author for correspondence (kerppola@umich.edu)

**Received 25 March 2014; Accepted 27 June 2014**

Development (2014) 141, 3277-3288 doi:10.1242/dev.110528

epoxide hydrolases can catalyze the degradation of juvenile hormone *in vitro* (Touhara and Prestwich, 1993; Khlebodarova et al., 1996), and their expression is correlated with specific developmental stages in insects (Seino et al., 2010). The mechanisms that coordinate the balance between ecdysone and juvenile hormone levels during different stages of development have not been identified.

Keap1 is predominantly cytoplasmic in cultured mammalian cells (Itoh et al., 1999; Watai et al., 2007). The interaction between Keap1 and Nrf2 has been proposed to inhibit Nrf2 transcriptional activity by confining Nrf2 to the cytoplasm, by facilitating Nrf2 export from the nucleus, and by inducing Nrf2 ubiquitylation and degradation (Itoh et al., 1999; McMahon et al., 2003; Kobayashi et al., 2004; Sun et al., 2007; Misra et al., 2011). The modification of selected cysteine residues in Keap1 by reactive oxygen species and by xenobiotic compounds has been proposed to block the effects of Keap1 on Nrf2 localization or ubiquitylation (Eggler et al., 2005; Kobayashi et al., 2009). This is thought to result in the accumulation of Nrf2 in the nucleus and the activation of xenobiotic response genes (Taguchi et al., 2011).

Nrf2 is required for the activation of different genes in response to different xenobiotic compounds in different mammalian cell lines and tissues (Thimmulappa et al., 2002; Kwak et al., 2003; Lee et al., 2003; Hu et al., 2006; Nair et al., 2006; Yates et al., 2009). The mechanisms that determine which genes are activated in response to different xenobiotic compounds have not been elucidated. We hypothesized that dKeap1 interacts with CncC on chromatin, and that xenobiotic compounds modulate their chromatin-binding specificities. To test this hypothesis, we used BiFC analysis to visualize interactions between dKeap1 and CncC on polytene chromosomes. Mapping the genetic loci bound by dKeap1-CncC complexes enabled the identification of genes that are selectively regulated by dKeap1-CncC complexes. Elucidating the effects of interactions between dKeap1 and CncC family proteins on their chromatin-binding specificities and on their transcriptional activities provided a new model for a mechanism that can mediate selective responses to different xenobiotic compounds and developmental signals.

## RESULTS

### Nuclear localization of dKeap1-CncC complexes in *Drosophila* tissues

The subcellular localization of protein complexes can provide insights into their functions. dKeap1 is localized to both the nucleus and the cytoplasm of cells in several different tissues (Fig. 1A; supplementary material Fig. S1A) (Deng and Kerppola, 2013). CncC is predominantly nuclear in all tissues that have been examined. To investigate interactions between dKeap1 and CncC in living tissues, we visualized dKeap1-CncC complexes in *Drosophila* larvae using BiFC analysis (Hu et al., 2002). dKeap1-CncC BiFC complexes were localized almost exclusively to the nuclei in living salivary gland cells (Fig. 1A). BiFC complexes formed by two different combinations of fusion proteins localized to the nucleoplasm and to subnuclear foci. The difference in subnuclear localization could be caused by the difference in the expression levels of these fusion proteins (supplementary material Fig. S2E). The nuclear localization of dKeap1-CncC BiFC complexes is likely to reflect the localization of endogenous dKeap1-CncC complexes, since endogenous dKeap1 and CncC were also localized to the nuclei in several cell types (supplementary material Fig. S1A) (Deng and Kerppola, 2013). dKeap1-CncC BiFC complexes were also localized to nuclei in diploid imaginal disc cells and in polyploid prothoracic gland cells (supplementary material Fig. S1B).

We investigated whether dKeap1 or CncC formed homodimers, and if their homodimerization affected their localization. BiFC complexes formed by dKeap1 homodimers were localized predominantly to the cytoplasm, whereas BiFC complexes formed by CncC homodimers were exclusively nuclear (Fig. 1A; supplementary material Fig. S1C). The non-overlapping distributions of dKeap1 homodimers and dKeap1-CncC complexes suggested that dKeap1-CncC complexes did not contain dKeap1 homodimers. This is in contrast to the hypothesis that mammalian Keap1 interacts with Nrf2 as a homodimer (Tong et al., 2006; Ogura et al., 2010).

To evaluate the specificity of BiFC complex formation by dKeap1 and CncC, we examined BiFC complex formation by dKeap1 and CncB, which lacks the N-terminal sequences that are homologous to those that mediate Nrf2 interaction with Keap1 (supplementary material Fig. S1D) (Veraksa et al., 2000). No fluorescence was detected in cells that expressed dKeap1 and CncB fused to fluorescent protein fragments (Fig. 1A). CncB-YC was expressed at a level that was intermediate between those of CncC-YN and CncC-YC, was localized to the nucleus and bound to chromatin (Fig. 1A; supplementary material Fig. S2C-E). BiFC complex formation by dKeap1 and CncC therefore required the N-terminal region of CncC.

### Chromatin binding by dKeap1-CncC complexes

To determine whether dKeap1 and CncC form complexes at specific chromatin loci, we adapted BiFC analysis to visualize dKeap1-CncC complexes on polytene chromosome spreads. Surprisingly, dKeap1-CncC BiFC complexes bound loci distinct from those that were bound by the individual dKeap1 and CncC proteins (Fig. 1B; supplementary material Fig. S1E). None of the loci that were bound by the BiFC complexes (e.g. 55F, 89E and 94E) was bound by both endogenous dKeap1 and CncC. Most of these loci were bound by low or undetectable levels of the dKeap1 and CncC fusion proteins when they were expressed separately (Fig. 1B, Fig. 2A,C; supplementary material Fig. S2A). Conversely, none of the loci that were bound by both endogenous dKeap1 and CncC had detectable BiFC fluorescence. In particular, no BiFC signal was detected at the ecdysone-inducible early puffs (e.g. 2B, 74EF and 75B). These puffs were bound prominently both by endogenous dKeap1 and CncC as well as by independently expressed dKeap1 and CncC fusion proteins (Fig. 1B, Fig. 2A,C; supplementary material Fig. S2A) (Deng and Kerppola, 2013). The BiFC complexes bound to fewer loci than either dKeap1 or CncC that were expressed separately, suggesting that dKeap1-CncC complexes bound chromatin with a higher specificity than either dKeap1 or CncC individually (Fig. 2C).

Neither dKeap1-dKeap1 nor CncC-CncC homodimer BiFC complexes were detected on polytene chromosomes, although the overall fluorescence intensities of these BiFC complexes were comparable to that of dKeap1-CncC BiFC complexes. All of the dKeap1 and CncC BiFC fusion proteins (dKeap1-YC, dKeap1-YN, CncC-YC and CncC-YN) bound to many of the same loci on chromatin (Fig. 2A; supplementary material Fig. S2A). These results suggest that BiFC complex binding on chromatin did not result from non-specific association between BiFC fusion proteins on chromatin.

### Effects of ectopic dKeap1 and CncC co-expression on their chromatin-binding specificities

The difference between the loci that were bound by dKeap1-CncC BiFC complexes versus dKeap1 and CncC expressed separately

Development (2014) 141, 3277-3288 doi:10.1242/dev.110528

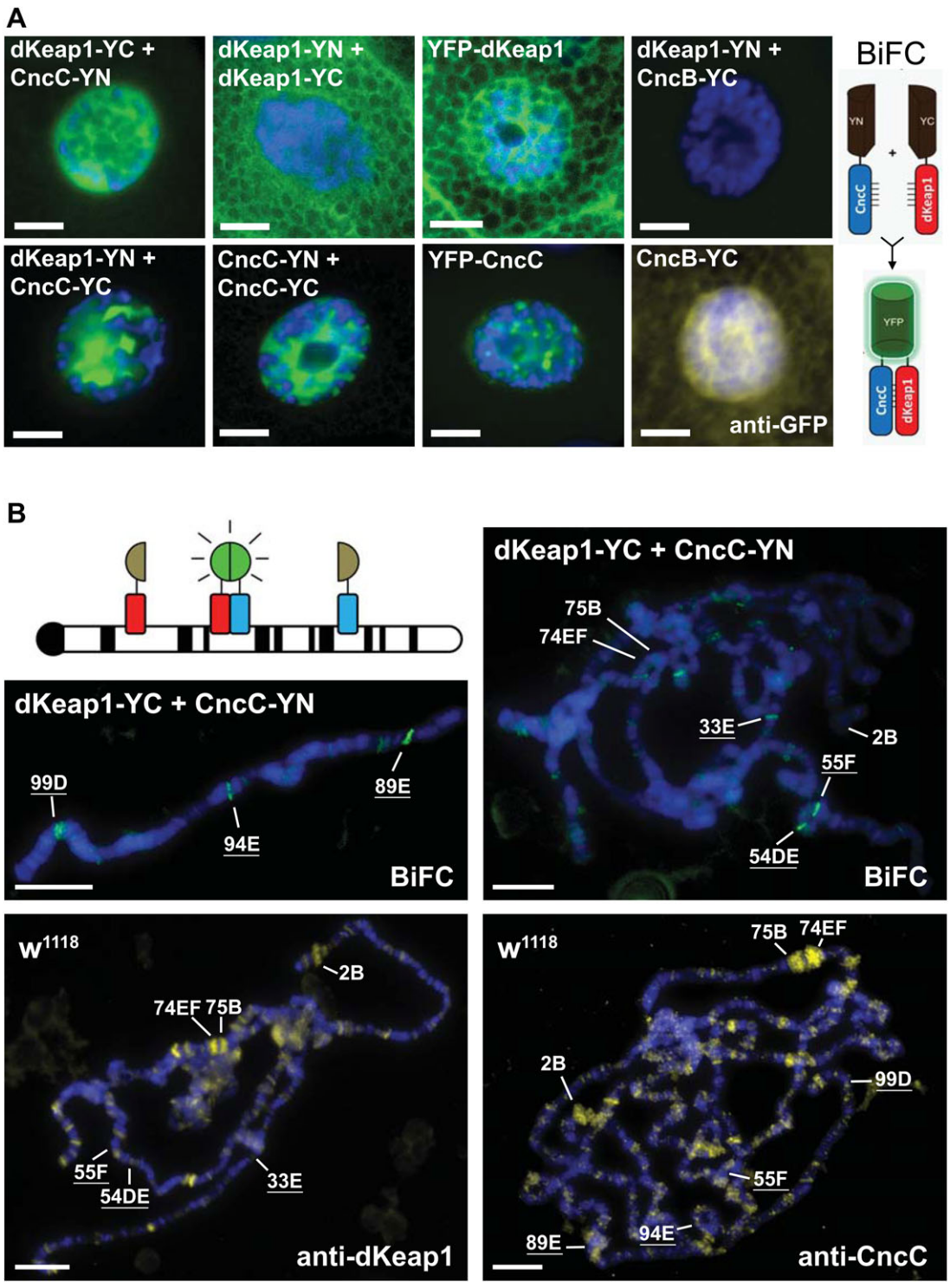


**Fig. 1. Subcellular localization and locus-specific polytene chromosome binding by dKeap1-CncC BiFC complexes.** (A) Subcellular localization of dKeap1-CncC, dKeap1-dKeap1 and CncC-CncC BiFC complexes and of the individual dKeap1 and CncC fusion proteins in *Drosophila* live salivary gland cells. The BiFC fusion proteins indicated in each image were expressed in salivary glands. The intrinsic BiFC and YFP fluorescence (green) were superimposed on Hoechst fluorescence (blue). CncB fusion protein localization was determined by immunostaining with anti-GFP antibodies (yellow). The fluorescence intensities of different cells varied over a wide range. The exposure times were adjusted to produce images of similar brightness. The subcellular distributions are representative of the majority of cells in each population. The diagram on the right depicts BiFC analysis. (B) Visualization of loci that are bound by dKeap1-CncC BiFC complexes and by endogenous dKeap1 and CncC on polytene chromosomes. (Top row) Intrinsic BiFC fluorescence was visualized on polytene chromosome spreads from larvae that expressed dKeap1-YC and CncC-YN. (Bottom row) Endogenous dKeap1 and CncC were visualized on polytene chromosomes from wild-type ($w^{1118}$) larvae by immunostaining. The BiFC (green), immunofluorescence (yellow) and Hoechst (blue) signals were superimposed. Selected loci that were bound by the BiFC complexes are underlined and loci that were predominantly bound by endogenous dKeap1 and CncC proteins are indicated without underlining. The diagram (top left) depicts BiFC analysis of complexes on a polytene chromosome. The binding patterns are representative of at least eight spreads from four separate experiments. Scale bars: 10 μm.

Development (2014) 141, 3277-3288 doi:10.1242/dev.110528

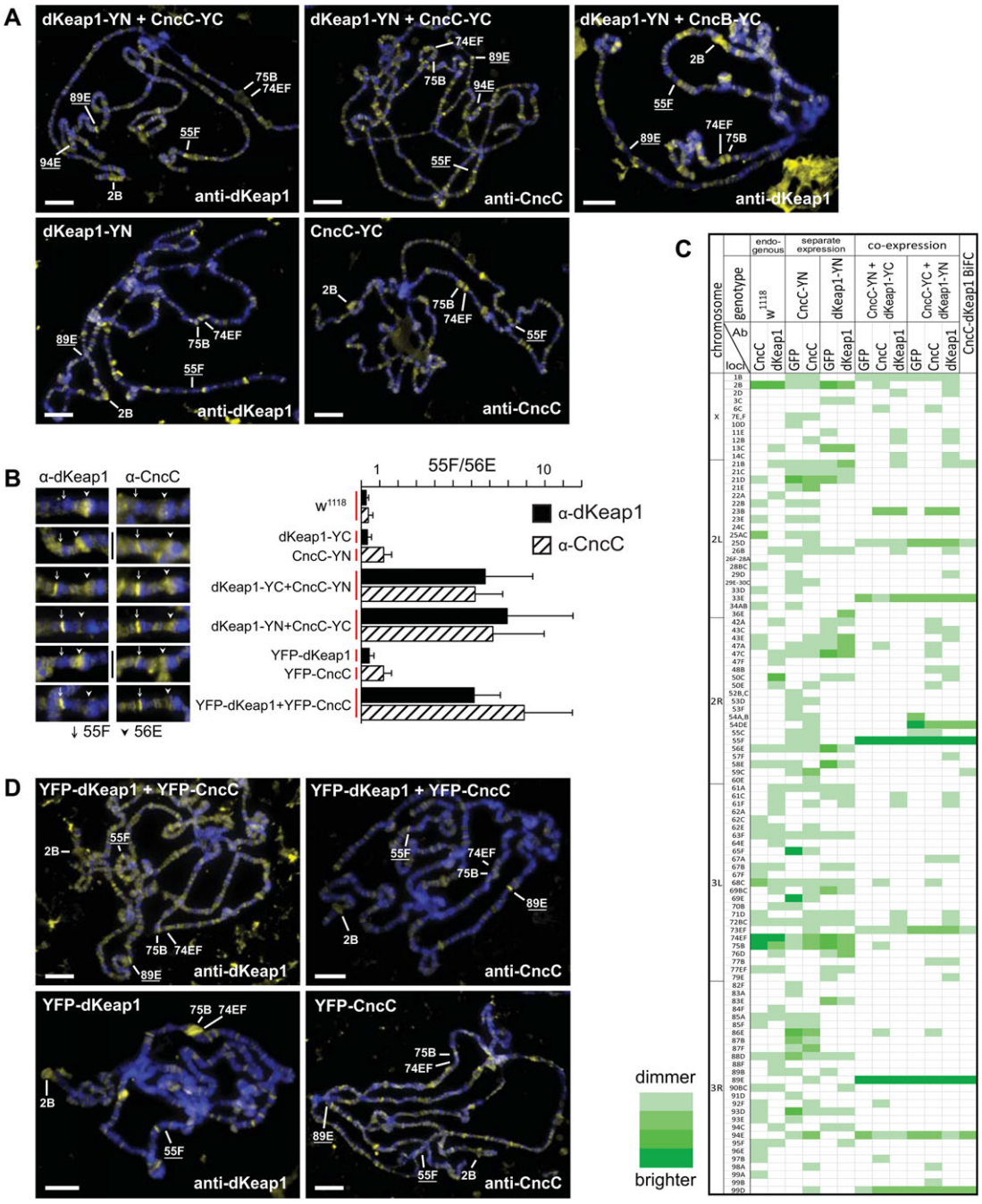


**Fig. 2. Effects of dKeap1 and CncC co-expression on their binding specificities on polytene chromosomes.** (A) Loci that were bound by dKeap1, CncC and CncB when they were co-expressed and when they were expressed separately. The proteins indicated at the top of each image were expressed in salivary glands. The loci that were bound by the fusion proteins were visualized by immunostaining (shown in yellow) using the antibodies indicated. Loci that were bound predominantly by co-expressed dKeap1 and CncC are underlined, whereas loci that were bound predominantly by dKeap1 and CncC that were expressed separately are indicated without underlining. The loci that were bound by different combinations of dKeap1 and CncC fusion proteins and polytene chromosome spreads that are stained with additional antibodies are shown in supplementary material Fig. S2A-C. (B) Quantitative analysis of dKeap1 and CncC binding specificities when they were co-expressed versus expressed separately. (Left) The images show sections of polytene chromosomes that were stained using the antibodies indicated. The fusion proteins that were expressed in the larvae are indicated to the right of the images. Horizontal pairs of images separated by a vertical bar were from larvae that expressed the dKeap1 and CncC fusion protein separately; the other pairs of images were from larvae that co-expressed both the dKeap1 and CncC fusion proteins. The top pair of images is from wild-type ($w^{1118}$) larvae. The 55F (arrow) and 56E (arrowhead) loci are indicated. (Right) The bar graph shows the average ratio (with s.d.) of the fluorescence intensities (55F/56E) from at least six spreads alongside the corresponding images. (C) Selected loci that were bound by endogenous dKeap1 and CncC, by dKeap1 and CncC fusion proteins expressed separately or in combination, and by dKeap1-CncC BiFC complexes. The intensities of the colored blocks indicate the relative levels of binding by each protein and complex at each locus. Only loci that had higher fluorescence intensities than the average intensity of all bands in the spread are indicated by the colored blocks. Thus, the absence of a colored block does not signify a lack of binding. (D) Loci that were bound by dKeap1 and CncC fused to intact fluorescent proteins expressed separately or in combination. The proteins as indicated at the top of each image were expressed in salivary glands. Polytene chromosome spreads were stained using the antibodies indicated. Selected loci are labeled as in A. The binding patterns in A and D are representative of at least ten separate images from three separate experiments. Scale bars: 10 μm.

Development (2014) 141, 3277-3288 doi:10.1242/dev.110528

could reflect selective BiFC complex formation at a subset of the loci that were bound by dKeap1 and CncC, or it could reflect a change in the selectivity of chromatin binding by dKeap1 and CncC when they were co-expressed. To distinguish between these possibilities, we compared the loci that were bound by the dKeap1 and CncC fusion proteins when they were expressed separately versus in combination. dKeap1 and CncC fusion proteins that were expressed separately bound most of the loci that were bound by endogenous dKeap1 and CncC (Fig. 2A; supplementary material Fig. S2A; e.g. 2B, 74EF and 75B). When the same fusion proteins were co-expressed, they bound preferentially to the loci that were bound by dKeap1-CncC BiFC complexes (Fig. 2, Fig. 1B; supplementary material Fig. S2A; e.g. 55F and 89E). The same change in binding specificities was detected by immunostaining with antibodies directed against dKeap1, CncC, as well as GFP (Fig. 2A,C; supplementary material Fig. S2A,B). Co-expression of dKeap1 and CncB fusion proteins, which did not form BiFC complexes, did not enhance their binding to the loci that were bound by dKeap1-CncC BiFC complexes (Fig. 2A; supplementary material Fig. S2C). Taken together, these results indicate that the difference between the loci that were bound by dKeap1-CncC BiFC complexes and those that were bound by dKeap1 and CncC independently reflects the effects of dKeap1-CncC interaction on their binding specificities.

To quantify the effect of dKeap1 and CncC co-expression on their binding specificities, we measured their relative levels of binding at neighboring loci when they were expressed separately and in combination. dKeap1 and CncC co-expression resulted in a reciprocal shift in their binding at the 55F and 56E loci compared with binding by endogenous dKeap1 and CncC as well as by ectopic dKeap1 expressed separately (Fig. 2B). Ectopic CncC expressed separately bound to many loci and exhibited little selectivity between the 55F and 56E loci. dKeap1 co-expression with CncC increased the selectivity of CncC binding between these loci and throughout the genome, suggesting that the dKeap1-CncC interaction enhanced the binding specificity of ectopic CncC.

We investigated whether BiFC complex formation or the protein fusions altered the binding specificities of dKeap1 and CncC. The same shift in binding was observed when dKeap1 and CncC fused to intact fluorescent proteins were co-expressed (Fig. 2D). BiFC complex formation was therefore not required for the effect that dKeap1 and CncC co-expression had on their binding specificities. Co-expression of dKeap1 and CncC fusion proteins containing either N- or C-terminal fusions caused the same changes in their binding specificities (Fig. 2A,D; supplementary material Fig. S2A). The positions of the protein fusions were therefore not important for the effects that dKeap1 and CncC co-expression had on their binding specificities.

We investigated the potential effects of differences in the levels of ectopic CncC and dKeap1 expression on their binding specificities by comparing the loci that were bound by CncC and dKeap1 fusion proteins that were expressed at different levels (supplementary material Fig. S2E). Co-expression of different dKeap1 and CncC fusion proteins caused the same changes in their binding specificities regardless of their expression levels (Fig. 2A; supplementary material Fig. S2A). It is therefore unlikely that differences in the levels of dKeap1 and CncC expression when they were expressed separately versus in combination caused the changes in their binding specificities.

All of the dKeap1 and CncC fusion proteins were expressed at higher levels than endogenous dKeap1 and CncC (supplementary material Fig. S2E). It is likely that the higher levels of ectopic dKeap1 and CncC co-expression caused the changes in their binding specificities as compared with the binding specificities of endogenous dKeap1 and CncC. We hypothesized that ectopic dKeap1 and CncC co-expression mimicked the effects of specific inducers of dKeap1 and CncC activity.

### Selective regulation of dKeap1 and CncC binding and of gene transcription by phenobarbital

To test the hypothesis that xenobiotic inducers of dKeap1 and CncC activity had effects similar to that of ectopic dKeap1 and CncC co-expression, we examined the effects of compounds that can activate xenobiotic response genes on dKeap1 and CncC binding on polytene chromosomes. CncC and Nrf2 are required for the induction of many xenobiotic response genes by phenobarbital and paraquat in adult *Drosophila* and by tBHQ in mammalian cells (Lee et al., 2003; Sykiotis and Bohmann, 2008; Misra et al., 2011). Paraquat can cause oxidative stress and is thought to activate Nrf2 through the oxidation of cysteine residues on Keap1 (Suntres, 2002). tBHQ can activate Nrf2 by increasing mitochondrial reactive oxygen species and the tBHQ metabolite *tert*-butylbenzoquinone can directly modify Keap1 (Imhoff and Hansen, 2010; Abiko et al., 2011). The mechanisms by which phenobarbital regulates Keap1-Nrf2 as well as dKeap1-CncC were not known.

Phenobarbital feeding induced endogenous dKeap1 binding at the 55F and 89E loci (Fig. 3A). The increase in dKeap1 binding at these loci was selective, as no dKeap1 binding was detected at loci containing other xenobiotic response genes (Fig. 3B; 47D, 51D, 55C, 87B) (Sykiotis and Bohmann, 2008; Misra et al., 2011). There was no detectable change in dKeap1 binding at other loci that were bound by dKeap1 in untreated larvae (Fig. 3A; 13C, 21B, 50C, 63F, 74EF). Phenobarbital feeding also increased the levels of ectopically expressed CncC binding at the 55F and 89E loci (supplementary material Fig. S3C). No endogenous CncC binding was detected at these loci, potentially because of the higher level of background staining of polytene chromosomes by anti-CncC antibodies.

Among the compounds tested, only phenobarbital induced dKeap1 and CncC binding at the 55F and 89E loci (Fig. 3C; supplementary material Fig. S3A). dKeap1 binding at other loci including 98E increased in larvae that were fed tBHQ, indicating that the lack of dKeap1 binding at the 55F and 89E loci in these larvae was not due to a failure of tBHQ feeding to influence dKeap1 binding (supplementary material Fig. S3B).

We examined the effects of phenobarbital, tBHQ and paraquat feeding on the transcription of genes at the loci that were bound by dKeap1-CncC BiFC complexes. *Juvenile hormone epoxide hydrolase 1* (*Jheh1*) and *Jheh2*, as well as the gene encoding endogenous dKeap, which are located at 55F and 89E, respectively, were induced in larvae that were fed phenobarbital (Fig. 3D,E). The level of *dKeap1* transcripts increased more rapidly than those of *Jheh* or other xenobiotic response genes, indicating that dKeap1 was probably activated directly in response to phenobarbital (Fig. 3E). The slower induction of other xenobiotic response gene transcripts indicates that their activation could be mediated in part by the *de novo* synthesis of other proteins, including dKeap1.

Phenobarbital feeding also activated the transcription of a subset of previously identified xenobiotic response genes, including *Cyp6a2*, *Cyp6a8*, *Cyp12d1* and *GstD2*, but did not activate other xenobiotic response genes (*GstD1* and *GstE1*) (Fig. 3D; supplementary material Fig. S3D). Phenobarbital activated most of the genes that were tested both in salivary glands and in whole larvae, suggesting that salivary glands were an appropriate model for the investigation of their regulation (Fig. 3D, Fig. 4A,B).

Development (2014) 141, 3277-3288 doi:10.1242/dev.110528

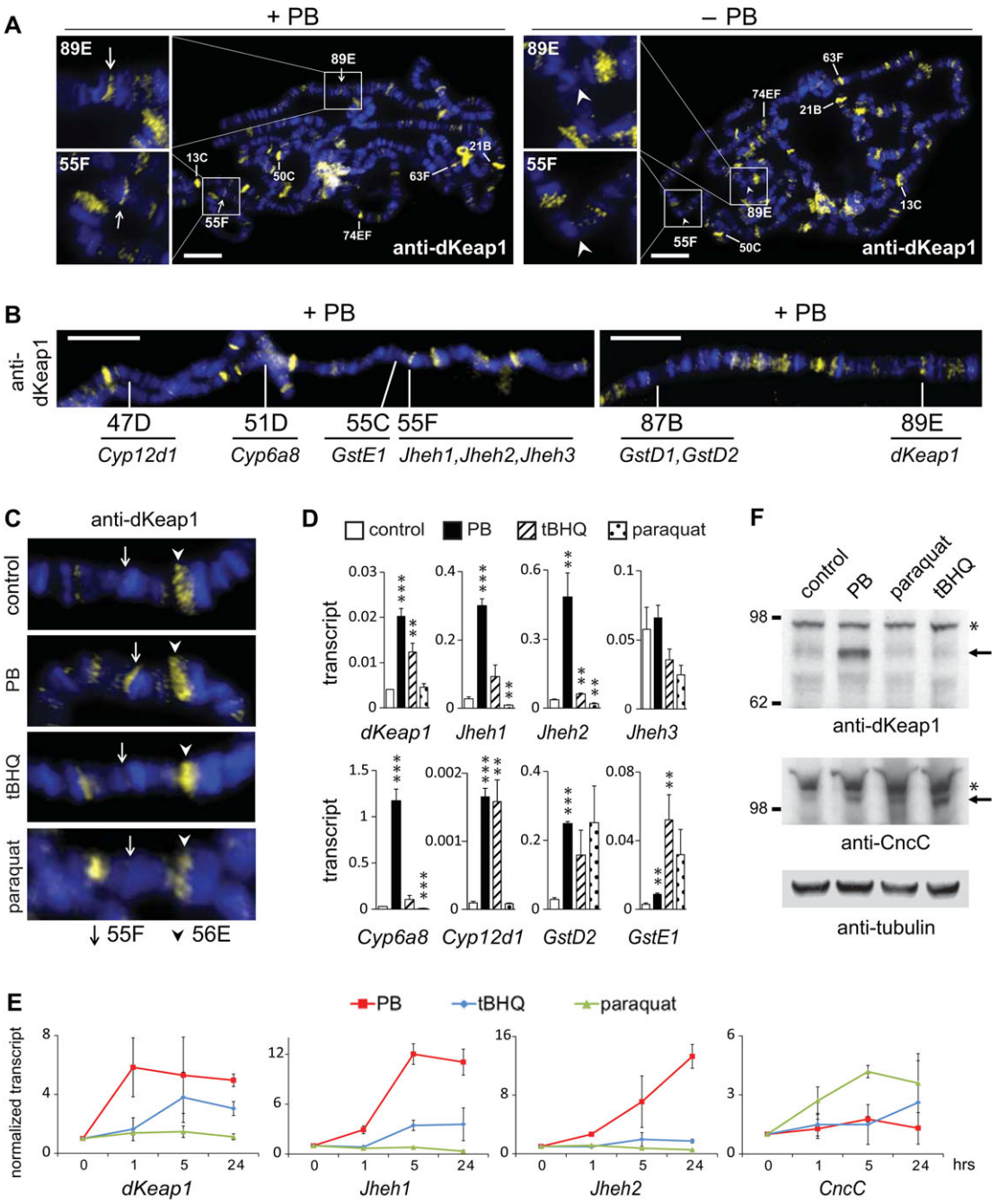


**Fig. 3. Effects of xenobiotic compounds on dKeap1 binding at selected loci on polytene chromosomes and on the transcription of xenobiotic response genes.** (A) Effects of phenobarbital feeding on the loci that were bound by dKeap1. Polytene chromosome spreads were prepared from larvae ($w^{1118}$) that were fed either phenobarbital (+PB) or control food (–PB) for 24 h, and were stained using antibodies against dKeap1. The immunostaining (yellow) and Hoechst (blue) signals were superimposed. Magnified views of the regions encompassing the 55F and 89E loci (arrows or arrowheads) are shown to the left of the spreads. The effects of phenobarbital feeding on CncC binding are shown in supplementary material Fig. S3C. (B) Effect of phenobarbital feeding on dKeap1 binding at loci encompassing known xenobiotic response genes. dKeap1 binding was examined at the indicated loci in larvae that were fed phenobarbital (+PB). Selected genes at each locus are indicated. (C) Effects of phenobarbital, tBHQ and paraquat feeding of larvae on dKeap1 binding at the 55F locus. Polytene chromosomes from third instar larvae that were fed phenobarbital, tBHQ paraquat or control food for 24 h were stained using anti-dKeap1 antibodies. Segments of polytene chromosomes containing the 55F (arrows) and 56E (arrowheads) loci are shown. The effects of these compounds on dKeap1 binding at additional loci are shown in supplementary material Fig. S3A,B. (D) Effects of phenobarbital, tBHQ and paraquat feeding on the transcription of *Jheh*, *dKeap1* and other xenobiotic response genes. Transcript levels were measured in four third instar larvae that were fed phenobarbital, tBHQ, paraquat or control food for 24 h. All transcript levels were normalized to the levels of *Rp49* (*RpL32*) transcripts. $^{**}P<0.05$, $^{***}P<0.01$ (ANOVA) for treated versus control groups from two separate experiments. Error bars indicate s.d. (E) Temporal changes in *dKeap1* and *Jheh* transcript levels following phenobarbital, tBHQ and paraquat feeding. Transcript levels were plotted relative to the levels of the same transcripts in larvae that were fed control food. All transcript levels were normalized to the levels of *Rp49* transcripts and represent the mean and s.d. from two separate experiments. The changes in the levels of additional transcripts are shown in supplementary material Fig. S3D. (F) Levels of endogenous dKeap1 and CncC proteins in larvae that were fed different xenobiotic compounds. Extracts of larvae that were fed control food or food containing phenobarbital, paraquat or tBHQ were analyzed by immunoblotting using the antibodies indicated. The bands corresponding to endogenous dKeap1 and CncC are indicated by arrows (asterisks indicate cross-reactive bands). Marker sizes (kDa) are indicated. Scale bars: 10 μm.

Development (2014) 141, 3277-3288 doi:10.1242/dev.110528

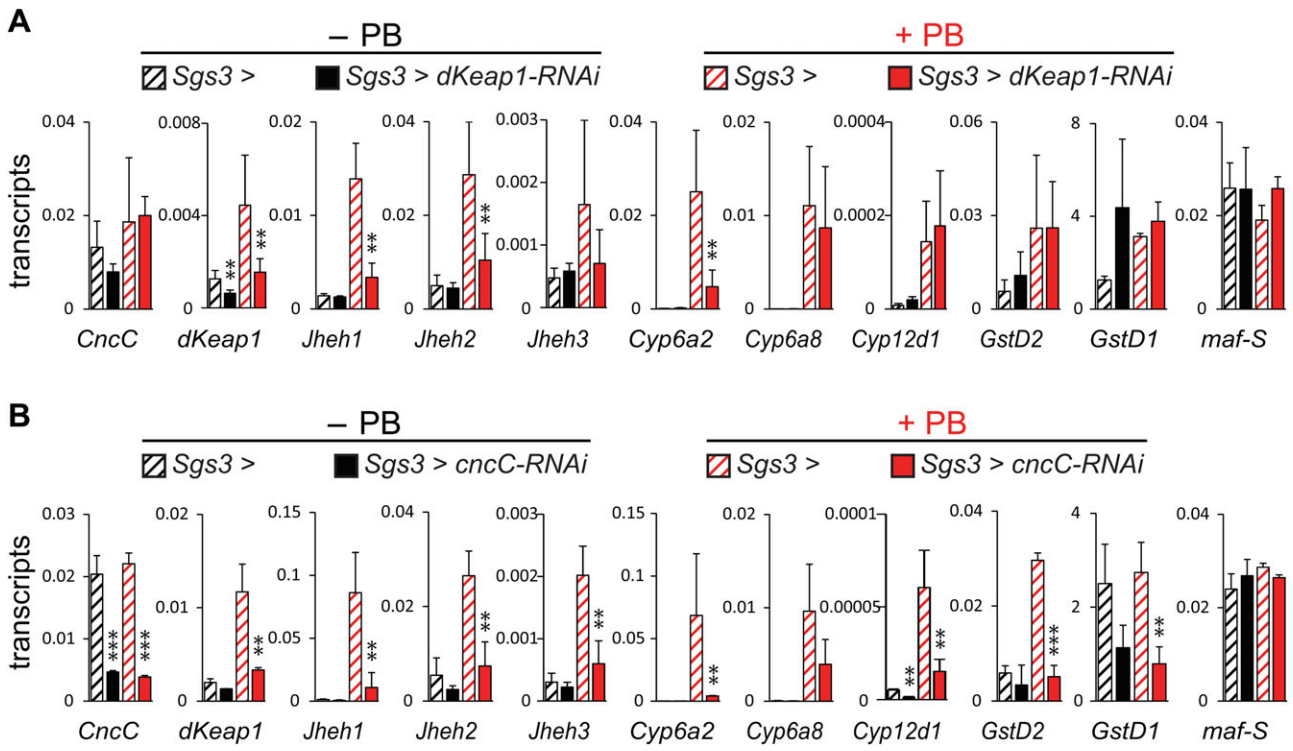


**Fig. 4. Roles of endogenous dKeap1 and CncC in phenobarbital activation of genes bound by dKeap1-CncC complexes and of other xenobiotic response genes.** Effects of dKeap1 (A) and of CncC (B) depletion on phenobarbital activation of different genes. Transcript levels were measured in ten pairs of salivary glands that expressed the indicated shRNAs and that were fed either phenobarbital (red bars) or control food (black bars) for 1 h. Larvae that expressed the shRNAs targeting *dKeap1* (*Sgs3 > dKeap1-RNAi*) or *cncC* (*Sgs3 > cncC-RNAi*) under the control of the *Sgs3-GAL4* driver (solid bars) were sorted from control larvae (*Sgs3 >*; striped bars) that were reared and analyzed in parallel. All transcript levels were normalized to the levels of *Rp49* transcripts. ***P*<0.05, ****P*<0.01 (ANOVA) for shRNA versus control groups from two separate experiments. Error bars indicate s.d.

Among the xenobiotic compounds tested, phenobarbital had the largest effects on *Jheh1*, *Jheh2* and *dKeap1* transcription as well as on dKeap1 binding at the 55F and 89E loci (Fig. 3D,C; supplementary material Fig. S3A). tBHQ had smaller effects on these transcripts and paraquat had no detectable effect, consistent with the undetectable levels of dKeap1 binding at the 55F and 89E loci in larvae that were fed tBHQ or paraquat. By contrast, tBHQ and paraquat had larger effects on dKeap1 binding as well as on transcription of several other xenobiotic response genes. Different xenobiotic compounds induced different combinations of the genes tested, suggesting that they activated these genes by distinct mechanisms.

We examined the effects of feeding different xenobiotic compounds on the levels of dKeap1 and CncC proteins. The level of dKeap1 increased in larvae that were fed phenobarbital, but not in those that were fed tBHQ or paraquat (Fig. 3F). By contrast, the level of CncC increased in larvae that were fed either phenobarbital, tBHQ or paraquat. The changes in dKeap1 and CncC levels suggested that phenobarbital activated genes that were bound by dKeap1-CncC complexes through a combination of transcriptional activation of *dKeap1* and post-transcriptional regulation of CncC levels.

### Roles of dKeap1 and CncC in phenobarbital induction of *Jheh* and *dKeap1* gene transcription

The observations that phenobarbital induced dKeap1 and CncC binding at the loci encompassing the *Jheh* and *dKeap1* genes and activated their transcription suggested that dKeap1 and CncC could mediate the activation of *Jheh* and *dKeap1* transcription by phenobarbital. We investigated the effects of endogenous dKeap1 and CncC depletion by shRNA expression on transcription of the *Jheh*, *dKeap1* and other xenobiotic response genes in larvae that were fed phenobarbital. Phenobarbital feeding increased transcription of *dKeap1*, *Jheh1*, *Jheh2*, *Jheh3* and many other xenobiotic response genes in salivary glands (Fig. 4). dKeap1 depletion reduced *Jheh1*, *Jheh2* and *Jheh3* transcription in the salivary glands of phenobarbital-fed larvae (Fig. 4A). By contrast, dKeap1 depletion had no significant effect on the transcription of other xenobiotic response genes tested, with the exception of *Cyp6a2*. dKeap1 was therefore required for phenobarbital activation of *Jheh* gene transcription, but it was not required for phenobarbital activation of most of the other xenobiotic response genes examined. CncC depletion reduced the levels of *Jheh1*, *Jheh2*, *Jheh3* and *dKeap1* as well as most other xenobiotic response gene transcripts in phenobarbital-fed larvae (Fig. 4B). Thus, both endogenous dKeap1 and CncC activated *Jheh* and *dKeap1* gene transcription in response to phenobarbital, whereas CncC, but not dKeap1, activated the transcription of most of the other xenobiotic response genes examined in phenobarbital-fed larvae.

### dKeap1 has opposite effects on CncC binding as well as on transcription at the *Jheh* and *dKeap1* versus other xenobiotic response genes

We investigated the combined effects of dKeap1 and CncC on chromatin binding and on transcriptional activation at genes that were bound by dKeap1-CncC complexes and at other xenobiotic response genes. Ectopically expressed CncC bound many loci, including those encompassing the *Jheh* and *dKeap1* genes as well those encompassing other xenobiotic response genes (Fig. 5A). Co-expression of ectopic dKeap1 with CncC enhanced CncC

Development (2014) 141, 3277-3288 doi:10.1242/dev.110528

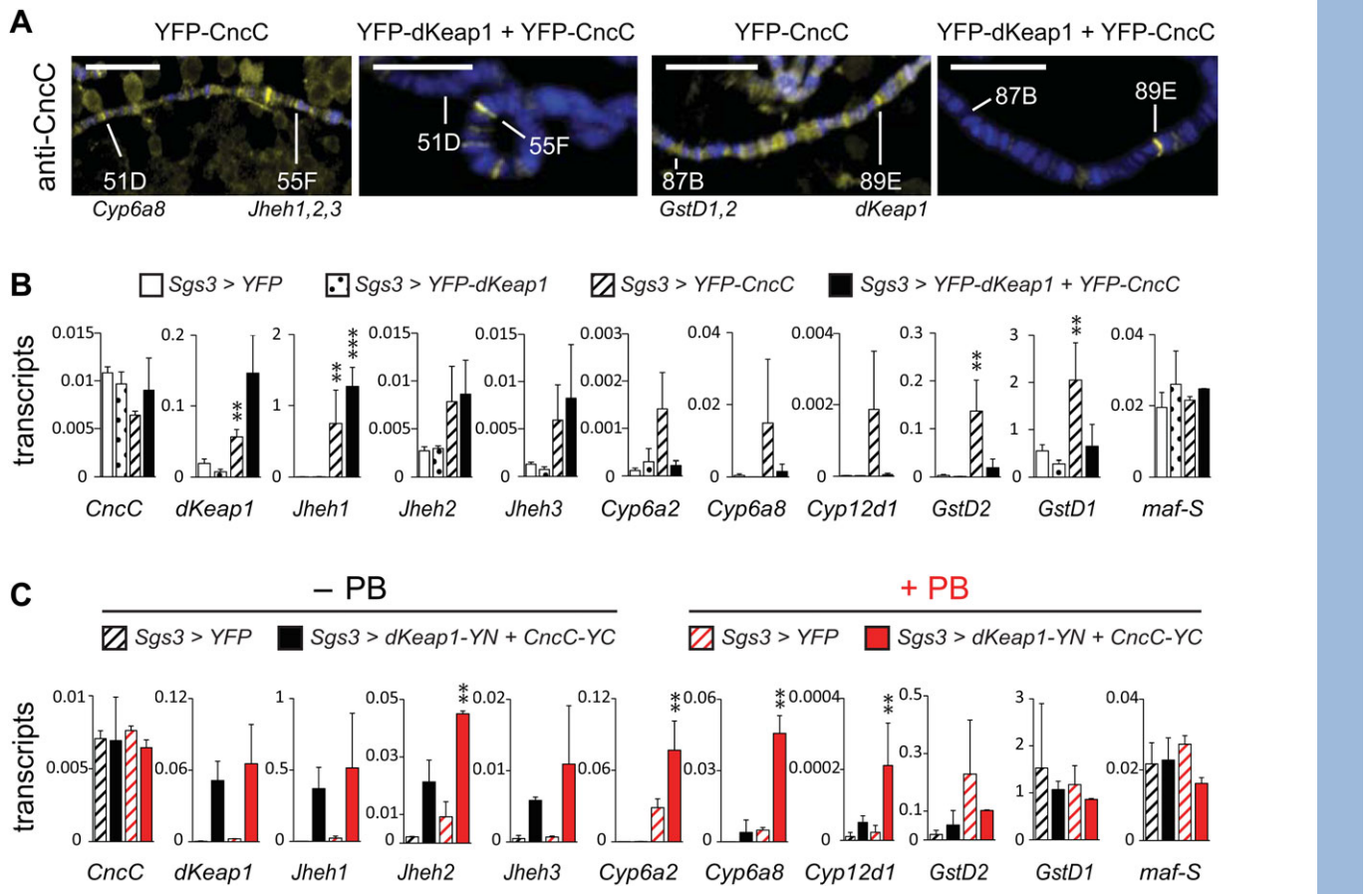


**Fig. 5. Effects of ectopic dKeap1 and CncC expression on transcription and on phenobarbital activation of genes bound by dKeap1-CncC complexes and of other xenobiotic response genes.** (A) CncC binding at selected loci when it was expressed separately versus co-expression with dKeap1. Sections of polytene chromosomes from larvae that expressed the fusion proteins indicated above each panel were stained using anti-CncC antibodies. Loci that encompass *Jheh* or *dKeap1* genes as well as other xenobiotic response genes are indicated. (B) Effects of ectopic dKeap1 and CncC expression separately and in combination on the transcription of different genes. Transcript levels were measured in ten pairs of salivary glands from larvae that expressed YFP or the dKeap1 and CncC fusion proteins indicated under the control of the *Sgs3-GAL4* driver. The effects of separate and combined expression of dKeap1 and CncC BiFC fusion proteins on transcription are shown in supplementary material Fig. S4. (C) Effects of ectopic dKeap1 and CncC co-expression on phenobarbital activation of different genes. Transcript levels were measured in ten pairs of salivary glands of third instar larvae that were fed either phenobarbital (red bars) or control food (black bars) for 1 h. Control larvae that expressed YFP and larvae that co-expressed dKeap1 and CncC fusion proteins were reared and analyzed in parallel. All transcript levels were normalized to the levels of *Rp49* transcripts. $^{**}P<0.05$, $^{***}P<0.01$ (ANOVA) for transgene versus control groups from two separate experiments. Error bars indicate s.d. Scale bars: 10 µm.

binding at the former loci, but suppressed CncC binding at the latter loci.

Ectopic CncC expression activated the transcription of *Jheh* and *dKeap1* as well as other xenobiotic response genes (Fig. 5B). Co-expression of dKeap1 with CncC further increased *Jheh1* and endogenous *dKeap1* gene transcription. By contrast, dKeap1 co-expression inhibited CncC activation of the other xenobiotic response genes examined. The same synergistic and antagonistic effects on transcription of these genes were observed when different dKeap1 and CncC fusion proteins containing either N- or C-terminal fusions were co-expressed (Fig. 5B; supplementary material Fig. S4). The different fusions did not therefore alter the effects of dKeap1 and CncC on transcription of the genes examined. Thus, ectopic dKeap1 co-expression with CncC had opposite effects on CncC binding as well as on transcriptional activation at the *Jheh* and *dKeap1* genes versus the other xenobiotic response genes.

We examined the combined effects of phenobarbital feeding and dKeap1-CncC co-expression on the transcription of these genes. Phenobarbital feeding of larvae that co-expressed dKeap1 and CncC in salivary glands did not further increase *Jheh* or *dKeap1* transcription (Fig. 5C). By contrast, phenobarbital feeding did increase the transcription of most of the other xenobiotic response genes examined in the salivary glands of these larvae. Ectopic dKeap1 and CncC bound the 55F and 89E loci and activated *Jheh* and *dKeap1* transcription at much higher levels than endogenous dKeap1 and CncC did in response to phenobarbital feeding (Fig. 5A, Figs 2 and 3). The distinct effects of ectopic dKeap1 and CncC co-expression on phenobarbital activation of *Jheh* and *dKeap1* versus other xenobiotic response genes are consistent with the hypothesis that dKeap1 and CncC regulate the transcription of these two groups of genes through distinct mechanisms.

### Effects of *Jheh* gene activation by dKeap1 and CncC co-expression on juvenile hormone-dependent functions

To test the hypothesis that dKeap1 and CncC regulate development by altering juvenile hormone levels through the activation of *Jheh* gene transcription, we examined the effects of dKeap1 and CncC co-expression on the timing of ommatidial development in pupae. When juvenile hormone was depleted by ablation of the corpus allatum premature ecdysone receptor expression was observed in the

Development (2014) 141, 3277-3288 doi:10.1242/dev.110528

eye disc (supplementary material Fig. S5A,B) (Riddiford et al., 2010; Riddiford, 2012). Conditional dKeap1 and CncC co-expression activated *Jheh1* and *Jheh2* transcription in third instar larvae and in pupae, but did not cause premature ecdysone receptor expression (supplementary material Fig. S5A,C,D). Ectopic dKeap1 and CncC expression also had no detectable effect on transcription of the *Kruppel homolog 1* (*Kr-h1*) gene, which is activated by juvenile hormone (supplementary material Fig. S5B-D) (Minakuchi et al., 2008). Ectopic dKeap1 and CncC co-expression in third instar larvae caused pupal lethality that was not suppressed by feeding the larvae with the juvenile hormone mimic methoprene. Thus, whereas dKeap1 and CncC co-expression induced *Jheh* gene transcription and arrested pupal development, it is likely that factors other than juvenile hormone depletion contributed to the pupal lethality.

## DISCUSSION

BiFC imaging of transcription factor interactions on polytene chromosomes provides a unique strategy for visualization of the genome-wide loci that are bound by combinatorial transcription regulatory complexes. The discoveries that dKeap1-CncC complexes are localized to nuclei and are bound to specific loci on polytene chromosomes challenge previous models for the effects of dKeap1 and CncC family protein interactions on their functions. The effects of dKeap1-CncC interaction on their chromatin-binding specificities and transcriptional activities have identified a combinatorial mechanism for the regulation of their functions that mediated selective gene activation by phenobarbital (Fig. 6).

### Chromatin-binding specificity of dKeap1-CncC complexes

The distinct loci bound by dKeap1-CncC BiFC complexes compared with the loci bound by dKeap1 and CncC expressed separately suggested that the interaction between dKeap1 and CncC altered their binding specificities. When dKeap1 and CncC were expressed separately, both proteins bound to the ecdysone response gene loci (Deng and Kerppola, 2013). However, they did not form BiFC complexes or enhance binding by each other at these loci. Three distinct modes of dKeap1 and CncC binding on chromatin were observed: (1) binding to the same loci without cooperative complex formation, as represented by the ecdysone response genes; (2) cooperative complex formation, as represented by the *Jheh* and *dKeap1* genes; and (3) independent binding to separate loci. These results indicate that multiple mechanisms, including cooperative DNA binding, influence the binding specificities and combinatorial regulation of transcription by dKeap1 and CncC.

Phenobarbital feeding induced endogenous dKeap1 and ectopic CncC binding at the *Jheh* and *dKeap1* loci, suggesting that phenobarbital induced dKeap1-CncC complex binding at these loci. The molecular mechanisms for the selective induction of dKeap1 and CncC binding at these loci remain to be fully characterized. The feed-forward loop produced by dKeap1-CncC complex activation of *dKeap1* gene transcription and the resulting increase in the level of dKeap1 protein is likely to be an integral component of this mechanism (Fig. 6).

### Selective binding and transcriptional activation by dKeap1-CncC

The selectivity of dKeap1-CncC BiFC complex formation at the *Jheh* and *dKeap1* loci correlated with the selectivity of dKeap1 activation of *Jheh* and *dKeap1* transcription in concert with CncC. The opposite effects of ectopic dKeap1 co-expression on ectopic CncC binding and on transcriptional activation at the *Jheh* and *dKeap1* genes versus other xenobiotic response genes are consistent with distinct mechanisms for the regulation of dKeap1 and CncC functions at different genes. Both endogenous dKeap1 and CncC activated *Jheh* gene transcription in phenobarbital-fed larvae. By contrast, CncC, but not dKeap1, mediated phenobarbital activation of the other xenobiotic response genes examined. Thus, dKeap1 and CncC synergistically activated the *Jheh* and *dKeap1* genes, whereas dKeap1 had an antagonistic effect on CncC activation of other xenobiotic response genes (Fig. 6). Phenobarbital feeding of larvae that expressed ectopic dKeap1 and CncC did not further activate *Jheh* or *dKeap1* transcription, whereas it activated other xenobiotic response genes. These results are consistent with the hypothesis that phenobarbital activates *Jheh* and *dKeap1* transcription by enhancing dKeap1-CncC complex formation at these loci, whereas phenobarbital activates other xenobiotic response genes by a distinct mechanism.

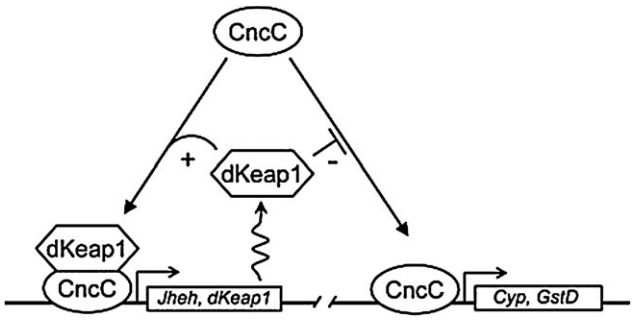


**Fig. 6. Model for the distinct effects of dKeap1 on CncC binding and on transcription at different genes.** dKeap1 and CncC enhance binding by each other (+) at some genes, resulting in synergistic activation of transcription. dKeap1 inhibits CncC binding (-) at other genes and represses their transcription. The activation of dKeap1 transcription by dKeap1-CncC amplifies the positive and negative regulatory responses.

### Feed-forward amplification of *dKeap1* transcription by dKeap1-CncC

The increased levels of *dKeap1* transcripts, dKeap1 protein and dKeap1 binding at the *dKeap1* locus in phenobarbital-fed larvae suggested that dKeap1 expression was regulated by a feed-forward loop (Fig. 6). The increase in *dKeap1* transcription preceded the increases in *Jheh* gene transcription, suggesting that the auto-activation of *dKeap1* transcription amplified the activation of other dKeap1-CncC target genes. The feed-forward activation of *dKeap1* transcription is likely to also modulate the activities of other xenobiotic response genes. Feed-forward loops regulate many developmental transitions and gene networks that maintain cellular states. Some inducers of Nrf2 activity can protect cells and organisms from subsequent exposure to toxic compounds and carcinogens (Liby et al., 2007; Kensler et al., 2013). In particular, phenobarbital pretreatment increases mouse resistance to parathion and reduces the incidence of chemically induced bladder cancer in rats (Vitarius et al., 1995). Feed-forward regulatory loops that activate dKeap1-CncC as well as Keap1-Nrf2 transcriptional networks could mediate such sensitization by xenobiotic agents.

### Selective effects of different xenobiotic compounds on dKeap1 and CncC binding and on transcription

dKeap1 and CncC binding and transcription at the *dKeap1* and *Jheh* genes were selectively enhanced by phenobarbital, but not by tBHQ

Development (2014) 141, 3277-3288 doi:10.1242/dev.110528

or paraquat. Different xenobiotic compounds also have distinct effects on the Nrf2-dependent transcriptomes in different mammalian cell lines and tissues (Thimmulappa et al., 2002; Kwak et al., 2003; Lee et al., 2003; Hu et al., 2006; Nair et al., 2006; Yates et al., 2009). The mechanisms that mediate the selective regulation of different genes in response to different xenobiotic compounds could involve differences in the formation and binding specificities of dKeap1-CncC, as well as of Keap1-Nrf2, complexes. The multiple mechanisms that can control the transcriptional activities of dKeap1 and CncC family protein complexes potentially provide many ways to coordinate transcriptional responses with different xenobiotic compounds and developmental signals.

### Visualization of combinatorial transcription complex binding specificity by BiFC imaging

The results of our experiments have established that genetic loci that are selectively bound by transcription factor complexes can be identified by mapping BiFC complex binding on polytene chromosomes. dKeap1 and CncC fusions formed BiFC complexes only at loci where dKeap1 and CncC bound cooperatively to chromatin, indicating that adventitious collisions between the fluorescent protein fragments did not facilitate BiFC complex formation. Thus, BiFC analysis can be used to identify differences between the binding specificities of protein complexes and those of their constituent subunits.

Ectopic overexpression of dKeap1 and CncC fusion proteins affected the loci that were bound by dKeap1 and CncC. In this case, ectopic dKeap1 expression mimicked the effect of feed-forward amplification of dKeap1 expression in response to selected xenobiotic compounds. In other situations, it might be necessary to control the levels of ectopic fusion proteins by using inducible expression vectors or endogenous promoters (Hudry et al., 2011). BiFC analysis has also been used to visualize Hox family transcription factor binding at a tandem array of integrated binding sites on polytene chromosomes (Papadopoulos et al., 2012). Our results demonstrate that at least some BiFC complexes bind to native loci that are bound and regulated by the endogenous proteins in response to specific stimuli.

Many biochemical, genetic, cell biological and computational approaches have been used to study combinatorial mechanisms of transcriptional regulation. Studies using different experimental approaches in different model systems have focused on different mechanisms of combinatorial transcriptional regulation (Arnosti et al., 1996; Burns and Kerppola, 2012; Takaya et al., 2012). BiFC analysis of protein interactions on polytene chromosomes combines various aspects of these approaches by providing information about molecular interactions in genetically modified animals at high spatial resolution. This strategy provides a unique and complementary approach for the investigation of regulatory processes on chromatin.

## MATERIALS AND METHODS

### *Drosophila* stocks

Plasmids encoding dKeap1, CncC and CncB fused to intact fluorescent proteins (rxYFP, here designated YFP) and fluorescent protein fragments (YN and YC) were constructed using the pUAST vector (Brand and Perrimon, 1993) and microinjected in the $w^{1118}$ background. Additional information about the plasmid expression vectors is available in the supplementary materials and methods. Lines that were not developed during this study were obtained from the Bloomington Stock Center, with the exception of the transgenic lines carrying *UAS-dKeap1-RNAi* and *UAS-cncC-RNAi*, which were generously provided by Dirk Bohmann (Sykiotis and Bohmann, 2008). Salivary gland expression was obtained using the *Sgs3-GAL4* driver line (Cherbas et al., 2003). All studies were conducted with larvae maintained at 25°C with the exception of larvae expressing BiFC fusion proteins, which were maintained at 21°C to enhance the polyploidy of salivary gland cells, and larvae carrying the *UAS-dKeap1-RNAi* transgene, which were maintained at 29°C to improve the efficiency of dKeap1 depletion.

### BiFC analysis of protein interactions on polytene chromosomes

Salivary glands that expressed BiFC fusion proteins were isolated from early wandering third instar larvae. Polytene chromosome spreads were prepared using an acid-free squash technique to avoid quenching of the BiFC fluorescence (Johansen et al., 2009). One pair of dissected salivary glands was incubated in freshly prepared 2% paraformaldehyde in Brower's Fixation Buffer (0.15 M PIPES, 3 mM $MgSO_4$, 1.5 mM EGTA, 1.5% NP40, pH 6.9) for 3 min, in PBST (PBS+0.2% Triton X-100) for 3 min, and in 50% glycerol for 5 min. The salivary glands were then squashed in 10 µl 50% glycerol and stained with Hoechst 33258 before mounting in 80% glycerol, 10 mM Tris pH 9.0. Live tissues were mounted in PBS and imaged within 5 min after dissection. Images were acquired on an Olympus IX81 inverted fluorescence microscope with a Hamamatsu ORCA-ER digital CCD camera. BiFC signal was visualized using 504 nm excitation and 542 nm emission wavelengths. The signals corresponding to each combination of excitation and emission wavelengths were pseudocolored and merged in RGB color space. Detailed experimental procedures related to BiFC analysis of protein interactions on polytene chromosomes are available in the supplementary materials and methods.

### Polytene chromosome immunostaining

Polytene chromosome spreads were prepared from salivary glands of early wandering third instar larvae using conventional squash and immunostaining protocols (Johansen et al., 2009). Whole salivary glands isolated from early wandering third instar larvae were immunostained as described (Phalle Bde, 2004). Antibodies used for immunostaining were: anti-GFP (Fitzgerald Industries, 20R-GR011; 1:200), anti-dKeap1 (1:100) and anti-CncC (1:100) (Deng and Kerppola, 2013), Alexa Fluor 594-conjugated goat anti-rabbit secondary antibody (Invitrogen, A-11012; 1:1000). The immunostained samples were mounted in VectaShield (Vector Laboratories). Additional information about the antisera and experimental procedures for polytene chromosome squash, immunostaining and imaging are available in the supplementary materials and methods.

### Xenobiotic compound feeding to larvae

Larvae were collected at third instar and were transferred to plates with Formula 24 *Drosophila* diet (Carolina Biological Supply) containing 0.1% phenobarbital (Sigma), 0.1% tBHQ (Sigma), 1% paraquat (Sigma) or water (control). Fewer than 20 larvae were placed on each plate to avoid overcrowding. After the indicated times, mRNA or protein was isolated and analyzed by RT-qPCR or immunoblotting. The sequences of the primers used for RT-qPCR are listed in supplementary material Table S1. Detailed experimental procedures for immunoblotting, transcript quantitation and statistical analyses of the data are available in the supplementary materials and methods.

#### Acknowledgements

We thank Sergei Avedisov for construction of the dKeap1, CncC and CncB expression vectors, Osamu Shimmi for preparing the *Drosophila* lines expressing dKeap1, CncC and CncB fusion proteins, Dirk Bohmann for *Drosophila* lines expressing shRNAs directed against *dKeap1* and *cncC*, Zhe Han for sharing equipment, and members of the T.K.K. laboratory for stimulating discussions.

#### Competing interests

The authors declare no competing financial interests.

#### Author contributions

H.D. and T.K.K. designed the project, planned the experiments, interpreted the data and wrote the paper. H.D. conducted the experiments.

#### Funding

This work was funded by the National Institutes of Health National Institute on Drug Abuse [DA030339] and National Institute of General Medical Sciences [GM086213]

and by a fellowship from the University of Michigan Center for Organogenesis to H.D. Deposited in PMC for release after 12 months.

### Supplementary material

Supplementary material available online at
http://dev.biologists.org/lookup/suppl/doi:10.1242/dev.110528/-/DC1

### References

**Abiko, Y., Miura, T., Phuc, B. H., Shinkai, Y. and Kumagai, Y.** (2011). Participation of covalent modification of Keap1 in the activation of Nrf2 by tert-butylbenzoquinone, an electrophilic metabolite of butylated hydroxyanisole. *Toxicol. Appl. Pharmacol.* **255**, 32-39.

**Arnosti, D. N., Barolo, S., Levine, M. and Small, S.** (1996). The eve stripe 2 enhancer employs multiple modes of transcriptional synergy. *Development* **122**, 205-214.

**Bai, S. and Kerppola, T. K.** (2011). Opposing roles of FoxP1 and Nfat3 in transcriptional control of cardiomyocyte hypertrophy. *Mol. Cell. Biol.* **31**, 3068-3080.

**Boube, M., Hudry, B., Immarigeon, C., Carrier, Y., Bernat-Fabre, S., Merabet, S., Graba, Y., Bourbon, H.-M. and Cribbs, D. L.** (2014). Drosophila melanogaster Hox transcription factors access the RNA polymerase II machinery through direct homeodomain binding to a conserved motif of mediator subunit Med19. *PLoS Genet.* **10**, e1004303.

**Brand, A. H. and Perrimon, N.** (1993). Targeted gene expression as a means of altering cell fates and generating dominant phenotypes. *Development* **118**, 401-415.

**Burns, V. and Kerppola, T. K.** (2012). Opposite orientations of a transcription factor heterodimer bind DNA cooperatively with interaction partners but have different effects on interferon-β gene transcription. *J. Biol. Chem.* **287**, 31833-31844.

**Cherbas, L., Hu, X., Zhimulev, I., Belyaeva, E. and Cherbas, P.** (2003). EcR isoforms in Drosophila: testing tissue-specific requirements by targeted blockade and rescue. *Development* **130**, 271-284.

**Deng, H. and Kerppola, T. K.** (2013). Regulation of Drosophila metamorphosis by xenobiotic response regulators. *PLoS Genet.* **9**, e1003263.

**Dubrovsky, E. B.** (2005). Hormonal cross talk in insect development. *Trends Endocrinol. Metab.* **16**, 6-11.

**Eggler, A. L., Liu, G., Pezzuto, J. M., van Breemen, R. B. and Mesecar, A. D.** (2005). Modifying specific cysteines of the electrophile-sensing human Keap1 protein is insufficient to disrupt binding to the Nrf2 domain Neh2. *Proc. Natl. Acad. Sci. USA* **102**, 10070-10075.

**ENCODE Project Consortium, Bernstein, B. E., Birney, E., Dunham, I., Green, E. D., Gunter, C. and Snyder, M.** (2012). An integrated encyclopedia of DNA elements in the human genome. *Nature* **489**, 57-74.

**Gohl, C., Banovic, D., Grevelhorster, A. and Bogdan, S.** (2010). WAVE forms hetero- and homo-oligomeric complexes at integrin junctions in Drosophila visualized by bimolecular fluorescence complementation. *J. Biol. Chem.* **285**, 40171-40179.

**Hu, C.-D., Chinenov, Y. and Kerppola, T. K.** (2002). Visualization of interactions among bZIP and Rel family proteins in living cells using bimolecular fluorescence complementation. *Mol. Cell* **9**, 789-798.

**Hu, R., Xu, C., Shen, G., Jain, M. R., Khor, T. O., Gopalkrishnan, A., Lin, W., Reddy, B., Chan, J. Y. and Kong, A. N.** (2006). Gene expression profiles induced by cancer chemopreventive isothiocyanate sulforaphane in the liver of C57BL/6J mice and C57BL/6J/Nrf2 (-/-) mice. *Cancer Lett.* **243**, 170-192.

**Hudry, B., Viala, S., Graba, Y. and Merabet, S.** (2011). Visualization of protein interactions in living Drosophila embryos by the bimolecular fluorescence complementation assay. *BMC Biol.* **9**, 5.

**Imhoff, B. R. and Hansen, J. M.** (2010). Tert-butylhydroquinone induces mitochondrial oxidative stress causing Nrf2 activation. *Cell Biol. Toxicol.* **26**, 541-551.

**Itoh, K., Wakabayashi, N., Katoh, Y., Ishii, T., Igarashi, K., Engel, J. D. and Yamamoto, M.** (1999). Keap1 represses nuclear activation of antioxidant responsive elements by Nrf2 through binding to the amino-terminal Neh2 domain. *Genes Dev.* **13**, 76-86.

**Jennings, P., Limonciel, A., Felice, L. and Leonard, M. O.** (2013). An overview of transcriptional regulation in response to toxicological insult. *Arch. Toxicol.* **87**, 49-72.

**Johansen, K. M., Cai, W., Deng, H., Bao, X., Zhang, W., Girton, J. and Johansen, J.** (2009). Polytene chromosome squash methods for studying transcription and epigenetic chromatin modification in Drosophila using antibodies. *Methods* **48**, 387-397.

**Kensler, T. W., Egner, P. A., Agyeman, A. S., Visvanathan, K., Groopman, J. D., Chen, J.-G., Chen, T.-Y., Fahey, J. W. and Talalay, P.** (2013). Keap1-nrf2 signaling: a target for cancer prevention by sulforaphane. *Top. Curr. Chem.* **329**, 163-177.

**Khlebodarova, T. M., Gruntenko, N. E., Grenback, L. G., Sukhanova, M. Z., Mazurov, M. M., Rauschenbach, I. Y., Tomas, B. A. and Hammock, B. D.** (1996). A comparative analysis of juvenile hormone metabolyzing enzymes in two species of Drosophila during development. *Insect Biochem. Mol. Biol.* **26**, 829-835.

**Kobayashi, A., Kang, M.-I., Okawa, H., Ohtsuji, M., Zenke, Y., Chiba, T., Igarashi, K. and Yamamoto, M.** (2004). Oxidative stress sensor Keap1 functions as an adaptor for Cul3-based E3 ligase to regulate proteasomal degradation of Nrf2. *Mol. Cell. Biol.* **24**, 7130-7139.

**Kobayashi, M., Li, L., Iwamoto, N., Nakajima-Takagi, Y., Kaneko, H., Nakayama, Y., Eguchi, M., Wada, Y., Kumagai, Y. and Yamamoto, M.** (2009). The antioxidant defense system Keap1-Nrf2 comprises a multiple sensing mechanism for responding to a wide range of chemical compounds. *Mol. Cell. Biol.* **29**, 493-502.

**Kwak, M.-K., Wakabayashi, N., Itoh, K., Motohashi, H., Yamamoto, M. and Kensler, T. W.** (2003). Modulation of gene expression by cancer chemopreventive dithiolethiones through the Keap1-Nrf2 pathway. Identification of novel gene clusters for cell survival. *J. Biol. Chem.* **278**, 8135-8145.

**Lee, J.-M., Calkins, M. J., Chan, K., Kan, Y. W. and Johnson, J. A.** (2003). Identification of the NF-E2-related factor-2-dependent genes conferring protection against oxidative stress in primary cortical astrocytes using oligonucleotide microarray analysis. *J. Biol. Chem.* **278**, 12029-12038.

**Liby, K., Royce, D. B., Williams, C. R., Risingsong, R., Yore, M. M., Honda, T., Gribble, G. W., Dmitrovsky, E., Sporn, T. A. and Sporn, M. B.** (2007). The synthetic triterpenoids CDDO-methyl ester and CDDO-ethyl amide prevent lung cancer induced by vinyl carbamate in A/J mice. *Cancer Res.* **67**, 2414-2419.

**Malhotra, D., Portales-Casamar, E., Singh, A., Srivastava, S., Arenillas, D., Happel, C., Shyr, C., Wakabayashi, N., Kensler, T. W., Wasserman, W. W. et al.** (2010). Global mapping of binding sites for Nrf2 identifies novel targets in cell survival response through ChIP-Seq profiling and network analysis. *Nucleic Acids Res.* **38**, 5718-5734.

**McGinnis, N., Ragnhildstveit, E., Veraksa, A. and McGinnis, W.** (1998). A cap 'n' collar protein isoform contains a selective Hox repressor function. *Development* **125**, 4553-4564.

**McMahon, M., Itoh, K., Yamamoto, M. and Hayes, J. D.** (2003). Keap1-dependent proteasomal degradation of transcription factor Nrf2 contributes to the negative regulation of antioxidant response element-driven gene expression. *J. Biol. Chem.* **278**, 21592-21600.

**McMahon, M., Thomas, N., Itoh, K., Yamamoto, M. and Hayes, J. D.** (2006). Dimerization of substrate adaptors can facilitate cullin-mediated ubiquitylation of proteins by a "tethering" mechanism: a two-site interaction model for the Nrf2-Keap1 complex. *J. Biol. Chem.* **281**, 24756-24768.

**Minakuchi, C., Zhou, X. and Riddiford, L. M.** (2008). Kruppel homolog 1 (Kr-h1) mediates juvenile hormone action during metamorphosis of Drosophila melanogaster. *Mech. Dev.* **125**, 91-105.

**Misra, J. R., Horner, M. A., Lam, G. and Thummel, C. S.** (2011). Transcriptional regulation of xenobiotic detoxification in Drosophila. *Genes Dev.* **25**, 1796-1806.

**Moi, P., Chan, K., Asunis, I., Cao, A. and Kan, Y. W.** (1994). Isolation of NF-E2-related factor 2 (Nrf2), a NF-E2-like basic leucine zipper transcriptional activator that binds to the tandem NF-E2/AP1 repeat of the beta-globin locus control region. *Proc. Natl. Acad. Sci. USA* **91**, 9926-9930.

**Nair, S., Xu, C., Shen, G., Hebbar, V., Gopalakrishnan, A., Hu, R., Jain, M. R., Lin, W., Keum, Y.-S., Liew, C. et al.** (2006). Pharmacogenomics of phenolic antioxidant butylated hydroxyanisole (BHA) in the small intestine and liver of Nrf2 knockout and C57BL/6J mice. *Pharm. Res.* **23**, 2621-2637.

**Nègre, N., Brown, C. D., Ma, L., Bristow, C. A., Miller, S. W., Wagner, U., Kheradpour, P., Eaton, M. L., Loriaux, P., Sealfon, R. et al.** (2011). A cis-regulatory map of the Drosophila genome. *Nature* **471**, 527-531.

**Ogura, T., Tong, K. I., Mio, K., Maruyama, Y., Kurokawa, H., Sato, C. and Yamamoto, M.** (2010). Keap1 is a forked-stem dimer structure with two large spheres enclosing the intervening, double glycine repeat, and C-terminal domains. *Proc. Natl. Acad. Sci. USA* **107**, 2842-2847.

**Papadopoulos, D. K., Skouloudaki, K., Adachi, Y., Samakovlis, C. and Gehring, W. J.** (2012). Dimer formation via the homeodomain is required for function and specificity of Sex combs reduced in Drosophila. *Dev. Biol.* **367**, 78-89.

**Phalle Bde, S.** (2004). Immunostaining of whole-mount imaginal discs. *Methods Mol. Biol.* **247**, 373-387.

**Pi, J., Leung, L., Xue, P., Wang, W., Hou, Y., Liu, D., Yehuda-Shnaidman, E., Lee, C., Lau, J., Kurtz, T. W. et al.** (2010). Deficiency in the nuclear factor E2-related factor-2 transcription factor results in impaired adipogenesis and protects against diet-induced obesity. *J. Biol. Chem.* **285**, 9292-9300.

**Plaza, S., Prince, F., Adachi, Y., Punzo, C., Cribbs, D. L. and Gehring, W. J.** (2008). Cross-regulatory protein-protein interactions between Hox and Pax transcription factors. *Proc. Natl. Acad. Sci. USA* **105**, 13439-13444.

**Riddiford, L. M.** (2012). How does juvenile hormone control insect metamorphosis and reproduction? *Gen. Comp. Endocrinol.* **179**, 477-484.

**Riddiford, L. M., Truman, J. W., Mirth, C. K. and Shen, Y.-C.** (2010). A role for juvenile hormone in the prepupal development of Drosophila melanogaster. *Development* **137**, 1117-1126.

**Seino, A., Ogura, T., Tsubota, T., Shimomura, M., Nakakura, T., Tan, A., Mita, K., Shinoda, T., Nakagawa, Y. and Shiotsuki, T.** (2010). Characterization of juvenile hormone epoxide hydrolase and related genes in the larval development of the silkworm Bombyx mori. *Biosci. Biotechnol. Biochem.* **74**, 1421-1429.

**Slocum, S. L. and Kensler, T. W.** (2011). Nrf2: control of sensitivity to carcinogens. *Arch. Toxicol.* **85**, 273-284.

**Sun, Z., Zhang, S., Chan, J. Y. and Zhang, D. D.** (2007). Keap1 controls postinduction repression of the Nrf2-mediated antioxidant response by escorting nuclear export of Nrf2. *Mol. Cell. Biol.* **27**, 6334-6349.
**Suntres, Z. E.** (2002). Role of antioxidants in paraquat toxicity. *Toxicology* **180**, 65-77.
**Sykiotis, G. P. and Bohmann, D.** (2008). Keap1/Nrf2 signaling regulates oxidative stress tolerance and lifespan in Drosophila. *Dev. Cell* **14**, 76-85.
**Taguchi, K., Motohashi, H. and Yamamoto, M.** (2011). Molecular mechanisms of the Keap1-Nrf2 pathway in stress response and cancer evolution. *Genes Cells* **16**, 123-140.
**Takaya, K., Suzuki, T., Motohashi, H., Onodera, K., Satomi, S., Kensler, T. W. and Yamamoto, M.** (2012). Validation of the multiple sensor mechanism of the Keap1-Nrf2 system. *Free Radic. Biol. Med.* **53**, 817-827.
**Thimmulappa, R. K., Mai, K. H., Srisuma, S., Kensler, T. W., Yamamoto, M. and Biswal, S.** (2002). Identification of Nrf2-regulated genes induced by the chemopreventive agent sulforaphane by oligonucleotide microarray. *Cancer Res.* **62**, 5196-5203.
**Tong, K. I., Katoh, Y., Kusunoki, H., Itoh, K., Tanaka, T. and Yamamoto, M.** (2006). Keap1 recruits Neh2 through binding to ETGE and DLG motifs: characterization of the two-site molecular recognition model. *Mol. Cell. Biol.* **26**, 2887-2900.
**Touhara, K. and Prestwich, G. D.** (1993). Juvenile hormone epoxide hydrolase. Photoaffinity labeling, purification, and characterization from tobacco hornworm eggs. *J. Biol. Chem.* **268**, 19604-19609.
**Tsai, J. J., Dudakov, J. A., Takahashi, K., Shieh, J.-H., Velardi, E., Holland, A. M., Singer, N. V., West, M. L., Smith, O. M., Young, L. F. et al.** (2013). Nrf2 regulates haematopoietic stem cell function. *Nat. Cell Biol.* **15**, 309-316.
**Venugopal, R. and Jaiswal, A. K.** (1996). Nrf1 and Nrf2 positively and c-Fos and Fra1 negatively regulate the human antioxidant response element-mediated expression of NAD(P)H:quinone oxidoreductase1 gene. *Proc. Natl. Acad. Sci. USA* **93**, 14960-14965.
**Veraksa, A., McGinnis, N., Li, X., Mohler, J. and McGinnis, W.** (2000). Cap 'n' collar B cooperates with a small Maf subunit to specify pharyngeal development and suppress deformed homeotic function in the Drosophila head. *Development* **127**, 4023-4037.
**Vincenz, C. and Kerppola, T. K.** (2008). Different polycomb group CBX family proteins associate with distinct regions of chromatin using nonhomologous protein sequences. *Proc. Natl. Acad. Sci. USA* **105**, 16572-16577.
**Vitarius, J. A., O'Shaughnessy, J. A. and Sultatos, L. G.** (1995). The effects of phenobarbital pretreatment on the metabolism and toxicity of paraoxon in the mouse. *Pharmacol. Toxicol.* **77**, 16-22.
**Wakabayashi, N., Itoh, K., Wakabayashi, J., Motohashi, H., Noda, S., Takahashi, S., Imakado, S., Kotsuji, T., Otsuka, F., Roop, D. R. et al.** (2003). Keap1-null mutation leads to postnatal lethality due to constitutive Nrf2 activation. *Nat. Genet.* **35**, 238-245.
**Watai, Y., Kobayashi, A., Nagase, H., Mizukami, M., McEvoy, J., Singer, J. D., Itoh, K. and Yamamoto, M.** (2007). Subcellular localization and cytoplasmic complex status of endogenous Keap1. *Genes Cells* **12**, 1163-1178.
**Yates, M. S., Tran, Q. T., Dolan, P. M., Osburn, W. O., Shin, S., McCulloch, C. C., Silkworth, J. B., Taguchi, K., Yamamoto, M., Williams, C. R. et al.** (2009). Genetic versus chemoprotective activation of Nrf2 signaling: overlapping yet distinct gene expression profiles between Keap1 knockout and triterpenoid-treated mice. *Carcinogenesis* **30**, 1024-1031.

**Figure S1**

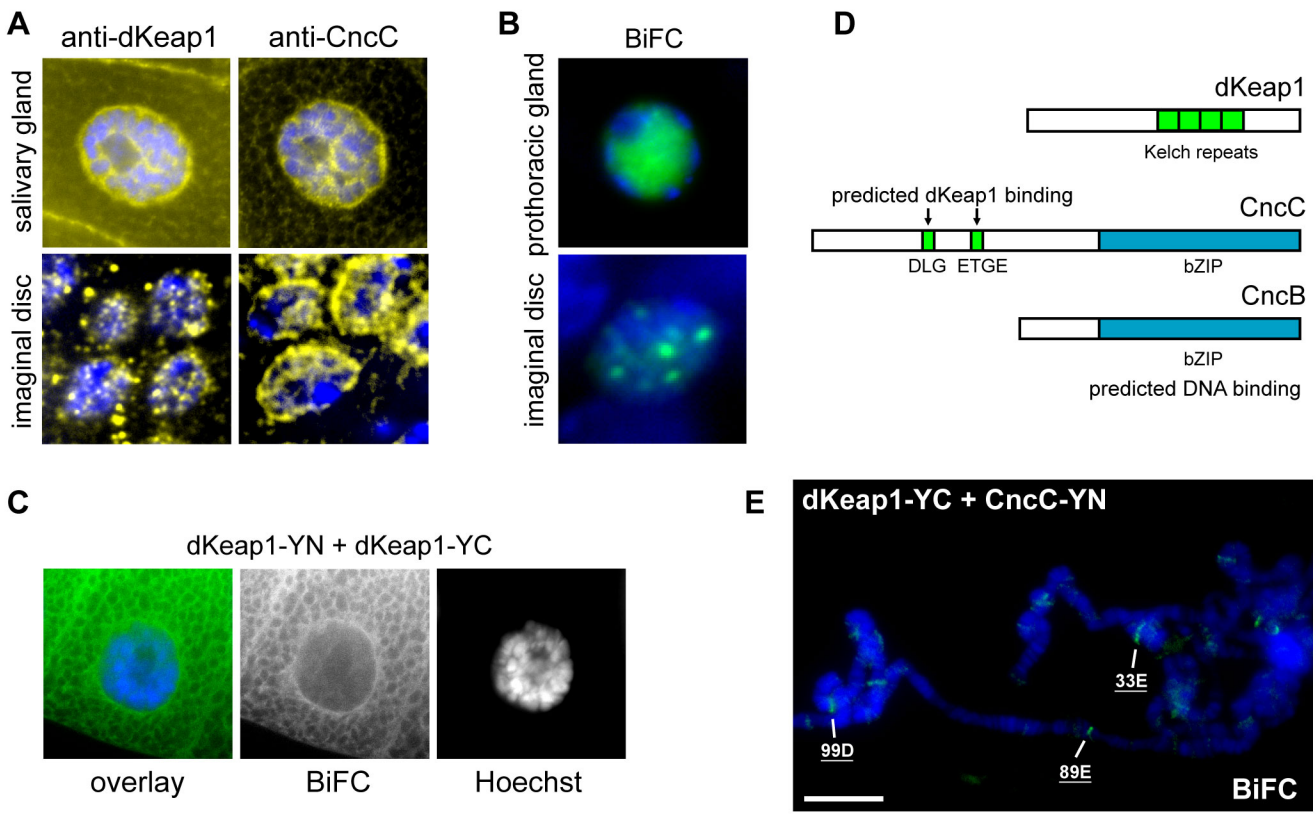
A
anti-dKeap1
anti-CncC
salivary gland
imaginal disc
B
BiFC
prothoracic gland
imaginal disc
D
dKeap1
Kelch repeats
predicted dKeap1 binding
CncC
DLG ETGE
bZIP
CncB
bZIP
predicted DNA binding
C
dKeap1-YN + dKeap1-YC
overlay
BiFC
Hoechst
E
dKeap1-YC + CncC-YN
33E
99D
89E
BiFC

**Figure S1. Subcellular localization of endogenous dKeap1 and CncC as well as of dKeap1-CncC BiFC complexes in different tissues**

**(A) Subcellular localization of endogenous dKeap1 and CncC in salivary gland and imaginal disc cells.** Salivary glands and wing imaginal discs from wild-type 3rd instar larvae were stained using antibodies raised against dKeap1 and CncC. The immunofluorescence (yellow) was superimposed on Hoechst fluorescence (blue).
**Interpretation:** Endogenous dKeap1 and CncC are predominantly nuclear in *Drosophila* tissues, consistent with the nuclear localization of ectopic dKeap1 and CncC in living cells (see Fig. 1A).

**(B) Visualization of dKeap1-CncC BiFC complexes in prothoracic gland and imaginal disc cells.** The intrinsic BiFC fluorescence was visualized in the prothoracic gland and in the wing imaginal disc from 3rd instar larvae that expressed the dKeap1 and CncC BiFC fusions indicated under the control of the *5015-GAL4* and *71B-GAL4* drivers, respectively. The *5015-GAL4* driver activates transcription in prothoracic glands and in salivary glands (Yoshiyama et al., 2006). The *71B-GAL4* driver activates transcription in imaginal discs and in salivary glands (Busson and Pret, 2007). The BiFC fluorescence (green) was superimposed on Hoechst fluorescence (blue).
**Interpretation:** The dKeap1-CncC BiFC complexes were present within the nuclei of polyploid prothoracic gland cells and diploid imaginal disc cells. Thus, dKeap1-CncC BiFC complexes were localized to the nuclei in different tissues and cell types (also see Fig. 1A).

**(C) Visualization of dKeap1-dKeap1 BiFC complexes in salivary gland cells.** The intrinsic BiFC fluorescence was visualized in salivary glands from 3rd instar larvae that expressed the dKeap1 BiFC fusions indicated under the control of the *Sgs3-GAL4* driver (Cherbas et al., 2003). The BiFC (green) and Hoechst fluorescence (blue) were superimposed and shown separately.
**Interpretation:** dKeap1 homodimers are localized almost exclusively to the cytoplasm, in contrast to the predominantly nuclear localization of dKeap1-CncC complexes as well as of endogenous dKeap1 and CncC (see Fig 1A and supplementary material Fig. S1A,B).

**(D). Diagrams of dKeap1, CncC and CncB.** Regions that are conserved between CncC and mammalian Nrf2 are shown in color. Regions that are predicted to mediate dKeap1-CncC interaction are shown in green.

**(E) Visualization of loci that are bound by dKeap1-CncC BiFC complexes on polytene chromosomes in larvae reared at higher temperature.** Intrinsic BiFC fluorescence was visualized on polytene chromosome spreads from larvae that expressed dKeap1-YC and CncC-YN. The larvae were reared at 29°C.
**Interpretation:** dKeap1 and CncC BiFC complexes bound the same loci in larvae that were reared at 29°C as in larvae that were reared at 21°C (Fig. 1B). The detailed conditions of fusion protein expression therefore did not influence the loci that were bound by the BiFC complexes.

**Figure S2**

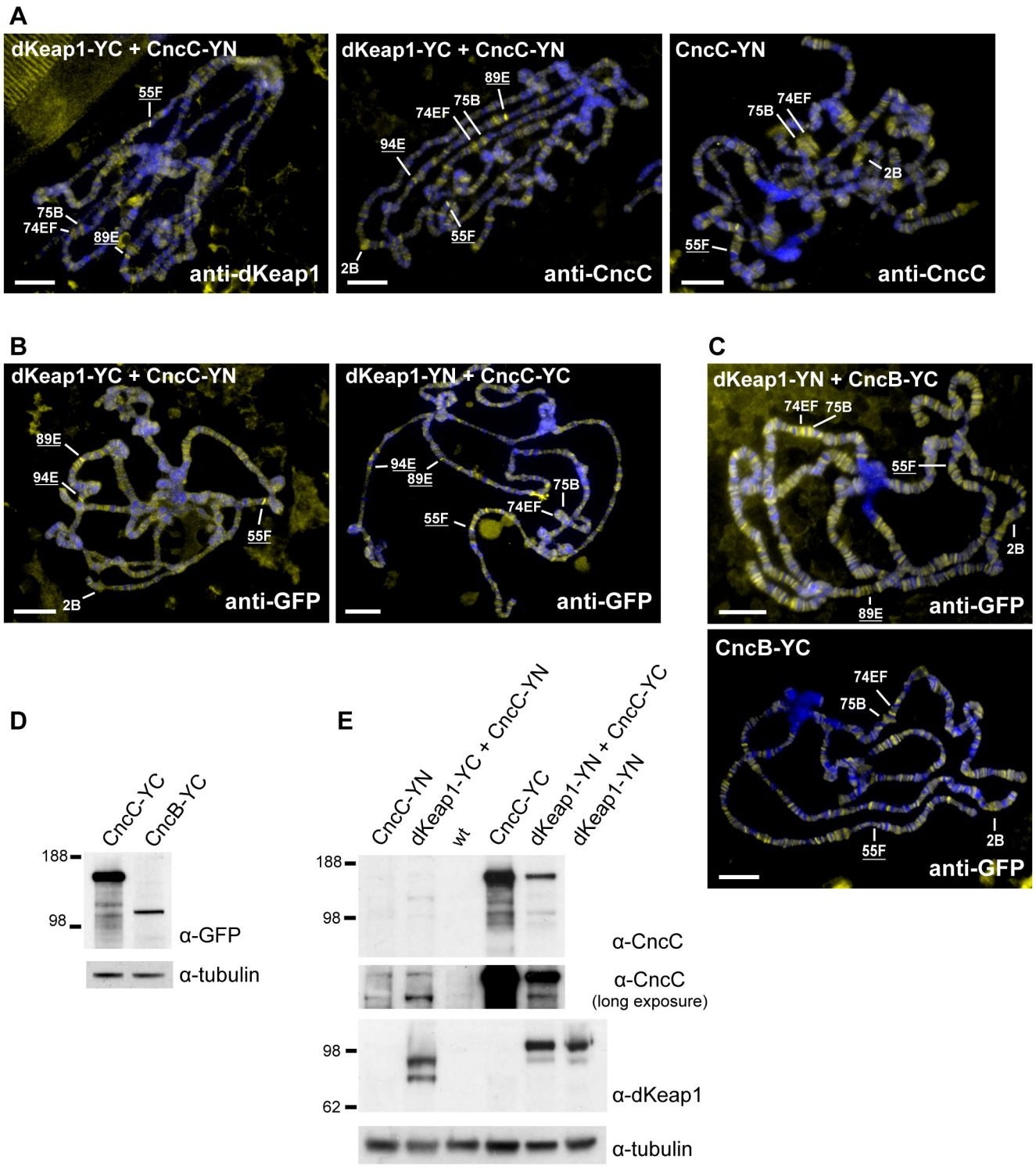
A
dKeap1-YC + CncC-YN
55F
75B
74EF
89E
anti-dKeap1
dKeap1-YC + CncC-YN
89E
75B
74EF
94E
55F
2B
anti-CncC
CncC-YN
74EF
75B
2B
55F
anti-CncC
B
dKeap1-YC + CncC-YN
89E
94E
55F
2B
anti-GFP
dKeap1-YN + CncC-YC
94E
89E
75B
74EF
55F
anti-GFP
C
dKeap1-YN + CncB-YC
74EF 75B
55F
2B
89E
anti-GFP
CncB-YC
74EF
75B
55F
2B
anti-GFP
D
CncC-YC
CncB-YC
188
98
α-GFP
α-tubulin
E
CncC-YN
dKeap1-YC + CncC-YN
wt
CncC-YC
dKeap1-YN + CncC-YC
dKeap1-YN
188
98
α-CncC
α-CncC
(long exposure)
98
62
α-dKeap1
α-tubulin

**Figure S2. Differences between the loci occupied by dKeap1 and CncC and their expression levels when they were co-expressed or expressed separately**

**(A) Loci occupied by dKeap1-YC and CncC-YN when they were co-expressed versus expressed separately.** Polytene chromosome spreads were prepared from larvae that expressed the fusion proteins indicated at the top of each panel in salivary glands under the control of the *Sgs3-GAL4* driver. The loci that were occupied by the fusion proteins were visualized by immunostaining using the antibodies indicated at the bottom of each panel. Immunofluorescence (yellow) was superimposed on Hoechst fluorescence (blue). The loci that were occupied by co-expressed CncC and dKeap1 (55F and 89E), as well as the ecdysone regulated puffs that were occupied by CncC and dKeap1 expressed separately (2B, 74EF, and 75B) are indicated on those polytene chromosome spreads where they could be mapped. The scale bars are 10 μm.
**Interpretation:** dKeap1 and CncC bound to distinct loci when they were co-expressed *versus* expressed separately. The same difference in binding was observed when different combinations of dKeap1 and CncC fusion proteins were expressed (dKeap1-YC + CncC-YN or dKeap1-YN + CncC-YC) (compare with Fig. 2A).

**(B) Detection of the loci occupied by co-expressed dKeap1 and CncC fusion proteins on polytene chromosomes by immunostaining using anti-GFP antibodies.** Polytene chromosome spreads from larvae that expressed the fusion proteins indicated at the top of each panel in salivary glands under the control of the *Sgs3-GAL4* driver were stained with antibodies against GFP.
**Interpretation:** The shift in binding upon dKeap1 and CncC co-expression was detected using antibodies directed against CncC, dKeap1 as well as GFP (compare with Fig. 2A,C).

**(C) Loci occupied by dKeap1 and CncB when they were co-expressed and by CncB when it was expressed separately.** Polytene chromosome spreads from larvae that expressed the fusion proteins indicated at the top of each panel in salivary glands under the control of the *Sgs3-GAL4* driver were stained using antibodies directed against GFP. Immunofluorescence (yellow) was superimposed on Hoechst fluorescence (blue).
**Interpretation:** CncB-YC occupied numerous loci that overlapped with the loci occupied by CncC-YC and CncC-YN, including 55F, 89E, 2B, 75B and 74EF (compare with Fig. 2A and S2A). Nevertheless, the CncB and CncC fusions did not occupy identical loci. Co-expression of dKeap1 and CncB fusions did not enhance their binding at the 55F and 89E loci in contrast to the co-expression of dKeap1 and CncC. Therefore, the change in binding produced by dKeap1 and CncC co-expression required direct interaction between the proteins.

**(D) Comparison of the levels of CncC and CncB fusion proteins.** Extracts from the salivary glands of larvae that carried the transgenes indicated above the lanes under the control of the *Sgs3-GAL4* driver were analyzed by immunoblotting using anti-GFP and anti-tubulin antibodies as indicated to the right of the blots.

**Interpretation:** The level of CncB-YC expression was lower than that of CncC-YC and higher than that of CncC-YN (see supplementary material Fig. S2E).

**(E) Comparison of the levels of CncC and dKeap1 fusion proteins expressed separately and in combination.** Extracts from control salivary glands and from salivary glands that carried the transgenes indicated abovethe lanes under the control of the *Sgs3-GAL4* driver were analyzed by immunoblotting using anti-CncC, anti-dKeap1 and anti-tubulin antibodies as indicated to the right of the blots.
**Interpretation:** The levels of expression of the CncC fusion proteins (CncC-YN *versus* CncC-YC) differed more than 10-fold. Nevertheless, co-expression of each of the CncC fusions with dKeap1 fusions (dKeap1-YN + CncC-YC and dKeap1-YC + CncC-YN) shifted the loci that were occupied by the CncC fusion proteins regardless of their levels of expression (see Fig. 2A, supplementary material Fig. S2A). Endogenous CncC was barely detectable, indicating that the levels of expression of the CncC fusion proteins were much higher than that of endogenous CncC.

**Figure S3**

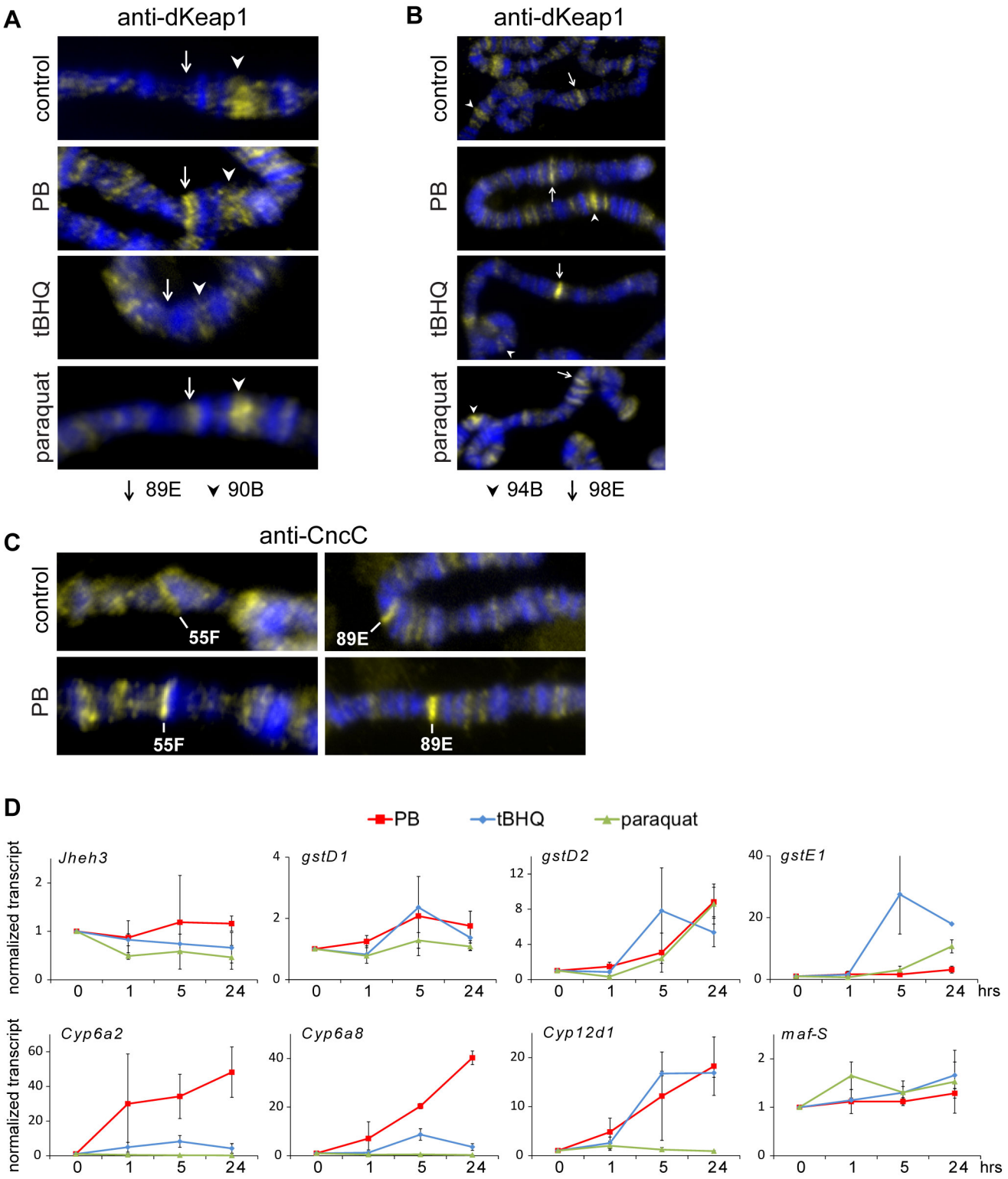
A
anti-dKeap1
control
PB
tBHQ
paraquat
89E
90B
B
anti-dKeap1
control
PB
tBHQ
paraquat
94B
98E
C
anti-CncC
control
PB
55F
89E
55F
89E
D
PB
tBHQ
paraquat
normalized transcript
Jheh3
gstD1
gstD2
gstE1
Cyp6a2
Cyp6a8
Cyp12d1
maf-S
0
1
5
24
hrs

**Figure S3. Effects of phenobarbital and other xenobiotic compounds on CncC occupancy and on xenobiotic response gene transcription**

**(A) Effects of phenobarbital, tBHQ, and paraquat feeding to larvae on dKeap1 binding at the 89E locus.** Polytene chromosomes from 3rd instar larvae that were fed phenobarbital (PB), tBHQ, paraquat or control food for 24 hours were stained using anti-dKeap1 antibodies. Segments of polytene chromosomes containing the 89E (arrows) and 90B (arrowheads) loci are shown.
**Interpretation:** Phenobarbital feeding increased endogenous dKeap1 binding at the 89E locus relative to the level of dKeap1 binding at the adjacent 90B locus. dKeap1 binding at the 89E locus in control larvae and in larvae that were fed tBHQ or paraquat was not detectable.

**(B) Effects of phenobarbital, tBHQ, and paraquat feeding to larvae on dKeap1 binding at the 98E locus.** Polytene chromosomes from 3rd instar larvae that were fed phenobarbital (PB), tBHQ, paraquat or control food for 24 hours were stained using anti-dKeap1 antibodies. Segments of polytene chromosomes containing the 98E (arrows) and 94B (arrowheads) loci are shown.
**Interpretation:** tBHQ feeding, but not phenobarbital or paraquat feeding, increased endogenous dKeap1 binding at the 98E locus relative to the level of dKeap1 binding at the adjacent 94B locus. The lack of dKeap1 binding at the 55F and 89E loci in these larvae was therefore not due to a failure of tBHQ feeding to influence dKeap1 binding.

**(C) Effects of phenobarbital feeding on ectopic CncC occupancy at the 55F and 89E loci.** Larvae that expressed CncC-YN in salivary glands under the control of the *Sgs3-GAL4* driver were fed phenobarbital (PB) or control food for 24 hours. Polytene chromosome spreads from these larvae were stained with antibodies against CncC.
**Interpretation:** Phenobarbital feeding increased ectopically expressed CncC binding at the 55F and 89E loci. No endogenous CncC binding was detected at the 55F or the 89E locus in control larvae or in larvae that were fed phenobarbital. The failure to detect endogenous CncC binding was potentially due to the higher level of background staining of polytene chromosomes by anti-CncC antibodies.

**(D) Effects of phenobarbital, tBHQ, and paraquat on xenobiotic response gene transcription at different times after feeding.** The transcripts indicated above the graphs were measured in 3rd instar larvae that were fed phenobarbital (PB, red lines), tBHQ (blue lines), paraquat (green lines) for 1, 5, or 24 hours. The levels of the transcripts indicated were normalized by the levels of the transcripts in larvae that were fed control food. The transcript levels were normalized by the levels of *Rp49* transcripts. The data shown represent the means and standard deviations from two separate experiments.
**Interpretation:** Phenobarbital, tBHQ, and paraquat feeding selectively activated the transcription of different genes at different times (compare with Fig. 3E).

**Figure S4**

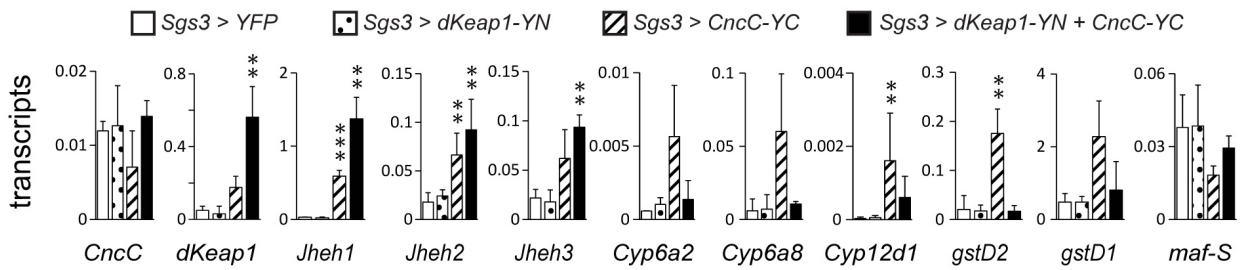


**Figure S4. Effects of ectopic dKeap1 and CncC expression on transcription of genes that are bound by dKeap1-CncC complexes and on that of other xenobiotic response genes**

**Comparison of the effects of dKeap1 and CncC BiFC fusion proteins expressed separately and in combination on transcription of different genes.** The levels of the transcripts indicated below the bar graphs were measured in the salivary glands of 3rd instar larvae. The transcripts were isolated from 10 pairs of salivary glands for each condition. All transcript levels were normalized by the levels of *Rp49* transcripts and correspond to the means and standard deviations from two separate experiments. The significance of the differences in transcription in transgenic *versus* control larvae was evaluated using ANOVA (**, $p<0.05$; ***, $p<0.01$).
**Interpretation:** The co-expression of ectopic dKeap1 and CncC fusion proteins synergistically activated transcription of the *Jheh* and *dKeap1* genes. In contrast, the co-expression of ectopic dKeap1 with CncC suppressed the activation of other xenobiotic response genes by CncC. The co-expression of different combinations of dKeap1 and CncC fusion proteins had consistently opposite effects on the transcription of these genes (also see Fig. 5B).

**Figure S5**

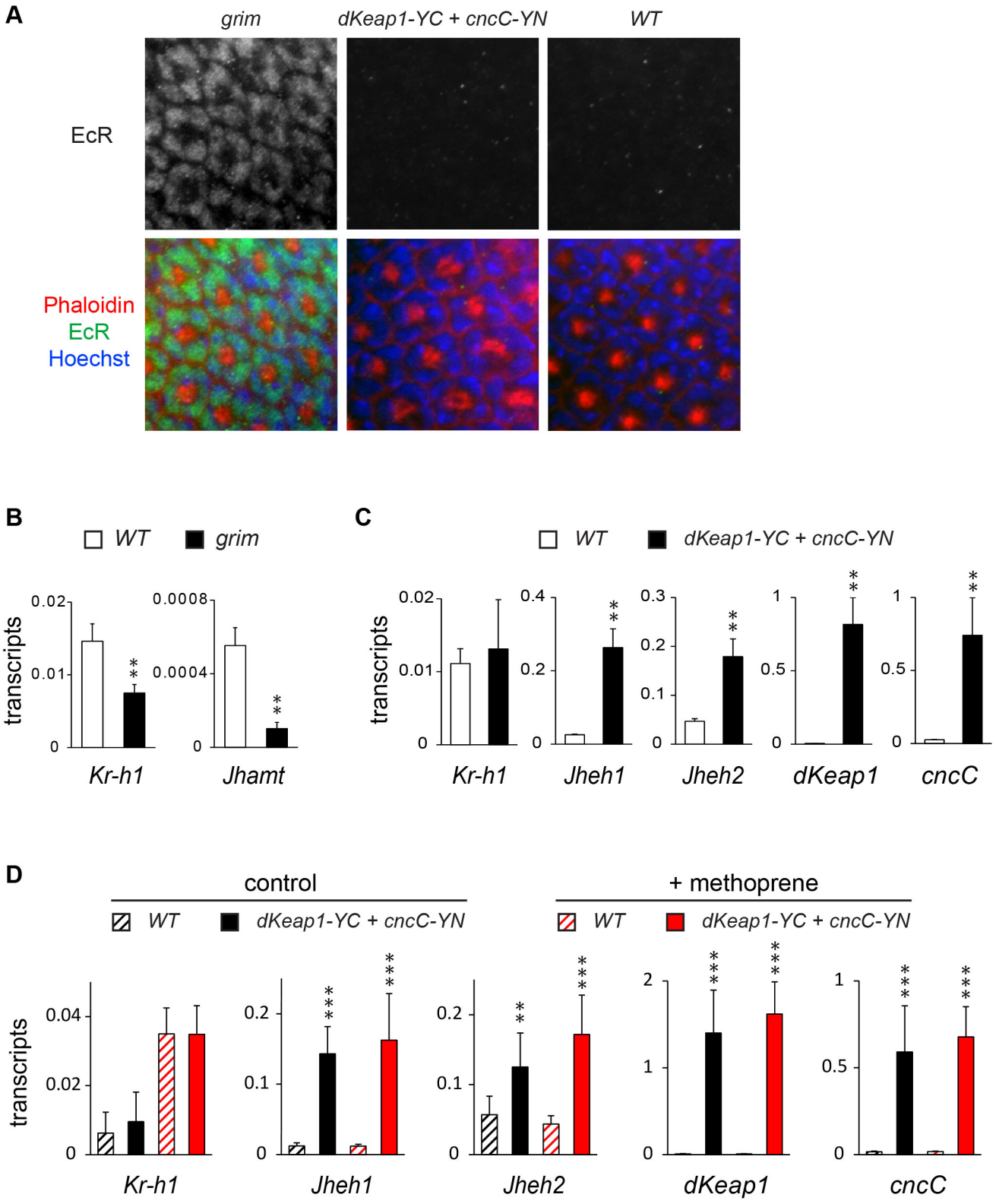
A
grim
dKeap1-YC + cncC-YN
WT
EcR
Phaloidin
EcR
Hoechst
B
WT
grim
transcripts
0.02
0.01
0
0.0008
0.0004
0
Kr-h1
Jhamt
C
WT
dKeap1-YC + cncC-YN
transcripts
Kr-h1
Jheh1
Jheh2
dKeap1
cncC
D
control
+ methoprene
WT
dKeap1-YC + cncC-YN
transcripts
0.04
0.02
0
0.2
0.1
Kr-h1
Jheh1
Jheh2
2
1
0.5
dKeap1
cncC

**Figure S5. Ectopic dKeap1 and CncC co-expression does not alter juvenile hormone-dependent functions**

**(A) Effects of dKeap1 and CncC co-expression, and of corpora allata ablation on the timing of ecdysone receptor expression in the optic disc.** Eye discs were isolated from pupae 2 hours after the pre-white pupae stage and immunolabeled as described (Phalle Bde, 2004). Ecdysone receptor (EcR) expression was compared between pupae that expressed *grim* under the control of the *Aug21-GAL4* driver (Mirth et al., 2005), pupae that co-expressed dKeap1 and CncC under the control of the *tubulin-GAL4 driver* and the temperature sensitive $GAL80^{ts}$ repressor (McGuire et al., 2004), and control pupae (WT). To inactive $GAL80^{ts}$, 3rd instar larvae were transferred from 19°C to 29°C 36 hours after molting. The developing ommatidia were counterstained using phalloidin. The EcR immunofluorescence (green), phalloidin (red) and Hoechst (blue) images were superimposed.
**Interpretation:** Ablation of the corpora allata by grim expression induced premature ecdysone receptor expression in the optic disc as shown previously (Riddiford et al., 2010). No ecdysone receptor expression was observed at this stage in control pupae or in pupae that co-expressed dKeap1 and CncC. dKeap1 and CncC co-expression and corpora allata ablation had distinct effects on EcR expression in the eye disc.

**(B) Effects of corpora allata ablation on Kr-h1 expression in the 3rd instar larvae.** The levels of the transcripts indicated above the graphs were measured in 3rd instar larvae that expressed *grim* under the control of the *Aug21-GAL4* driver (grim) and control larvae (WT), and were normalized by the levels of *Rp49* transcripts. The data shown represent the means and standard deviations from two separate experiments. The significance of the differences in the transcript levels between grim transgenic and control pupae was determined by using ANOVA (**, $p<0.05$).
**Interpretation:** *Jhamt* is a juvenile hormone biosynthetic gene that is specifically expressed in the corpora allata. The decrease in *Jhamt* transcription is consistent with ablation of the corpora allata by grim expression. The decrease in the level of *Kr-h1* transcripts upon corpora allata ablation suggests that juvenile hormone enhances *Kr-h1* transcription in 3rd instar larvae.

**(C) Effects of dKeap1-CncC co-expression on Jheh and Kr-h1 transcription.** The levels of the transcripts indicated below the bar graphs were measured in 3rd instar larvae that co-expressed dKeap1 and CncC under the control of the *Tubulin-GAL4* driver and the temperature-sensitive $GAL80^{ts}$ repressor (solid bars) as well as in control larvae (open bars). Larvae were collected 24 hours after transferring them from 19°C to 29°C to inactivate $GAL80^{ts}$. All transcript levels were normalized by the levels of *Rp49* transcripts. The data shown represent the means and standard deviations from two separate experiments. The significance of the differences in transcript levels between transgenic and control larvae was evaluated by ANOVA (***, $p<0.01$).
**Interpretation:** The levels of *Jheh1* and *Jheh2* transcripts were induced by conditional dKeap1 and CncC fusion protein co-expression. No change in *Kr-h1* transcripts was detected in these larvae.

**(D) Effects of methoprene administration and dKeap1-CncC co-expression on Jheh and Kr-h1 transcription.** 3rd instar larvae that co-expressed dKeap1 and CncC under the control of the *Tubulin-GAL4* driver and the temperature-sensitive *GAL80$^{ts}$* repressor (solid bars) as well as the control larvae (striped bars) were transferred from 19°C to 29°C 36 hours after molting. White pre-pupae derived from these larvae were treated with 0.2 µl of 0.3% methoprene, a juvenile hormone mimic, in acetone (red bars) or acetone alone (black bars). The levels of the transcripts indicated below the graphs were measured in pupae 24 hours after pupation, and were normalized by the levels of *Rp49* transcripts. The data shown represent the means and standard deviations from five separate experiments. The significance of the differences in transcript levels between transgenic and control pupae were tested by ANOVA (**, $p<0.05$; ***, $p<0.01$).
**Interpretation:** The level of *Kr-h1* transcripts was increased by methoprene. It was not affected by dKeap1 and CncC co-expression in pupae, whereas *Jheh1* and *Jheh2* transcripts were induced.

## Supplementary Materials and Methods

### Plasmid expression vectors

The dKeap1-YN and CncC-YN expression vectors encoded residues 1-173 of YFP fused to the C-termini of dKeap1 and CncC, respectively, in pUAST (Brand and Perrimon, 1993). The dKeap1-YC, CncC-YC and CncB-YC expression vectors encoded residues 174-238 of YFP fused to the C-termini of dKeap1, CncC and CncB, respectively, in pUAST. The YFP-dKeap1 and YFP-CncC expression vectors encoded rxYFP fused to the N-termini of dKeap1 and CncC, respectively, in pUAST. rxYFP contains the N149C and S202C substitutions in YFP (Ostergaard et al., 2001).

### BiFC analysis of protein interactions on polytene chromosomes

Salivary glands that expressed BiFC fusion proteins were isolated from early wandering 3rd instar larvae that were reared at 21°C to enhance the polyploidy of salivary gland cells (Johansen et al., 2009). Polytene chromosome spreads were prepared using an acid-free squash technique to avoid quenching of the BiFC fluorescence (Johansen et al., 2009). One pair of salivary glands was dissected in PBS and then incubated in freshly prepared 2% paraformaldehyde in Brower's Fixation Buffer (0.15 M PIPES, 3 mM $MgSO_4$, 1.5 mM EGTA, 1.5% NP40, pH6.9) for 3 minutes, in PBST (PBS + 0.2% Triton X-100) for 3 minutes, and in 50% glycerol allowing to soak for 5 minutes. The salivary glands were then transferred to 10 µl of 50% glycerol, and squashed between a coverslip coated with Sigmacote (Sigma) and a microscope slide coated with poly-lysine (Sigma). The slides were frozen in liquid nitrogen and the coverslips were removed using a razor blade immediately after taking them from the liquid nitrogen. The slides were incubated in PBS for 15 min followed by staining with Hoechst 33258 (Molecular Probes) in PBS for 10 minutes. The preparations were then washed with PBS for 5 minutes, dried, and mounted in 80% glycerol containing 10 mM Tris pH 9.0. All images were acquired on Olympus IX81 inverted fluorescence microscope with a Hamamatsu ORCA-ER digital CCD camera. BiFC signal was visualized using 504 nm excitation and 542 nm emission wavelengths. The signals corresponding to each combination of excitation and emission wavelengths were pseudocolored and merged in RGB color space.

### Antisera, conventional polytene chromosome squash, immunostaining and imaging

Anti-dKeap1 and anti-CncC antisera were raised against proteins encompassing residues 620-776 of dKeap1 and residues 88-344 of CncC fused to GST. The antisera were affinity purified by incubating them with Nitrocellulose membranes with dKeap1 or CncC fusion proteins, followed by elution.

Polytene chromosome squashes were prepared by dissecting 2-3 pairs of salivary glands and fixing them in freshly prepared 200 µl PBS + 4% paraformaldehyde + 1% Triton X-100 for 1 minute followed by incubation in freshly prepared 200 µl 45% acetic acid + 4% paraformaldehyde for 2 minutes. The fixed salivary glands were transferred to 10 µl 16.7% lactoacetic acid + 25% acetic acid and squashed between a coverslip coated with Sigmacote (Sigma) and a microscope slide coated with poly-lysine (Sigma) as described in detail in Johansen et al. (2009). The polytene

chromosome squashes were immuno-labeled as described (Johansen et al., 2009; Silver and Elgin, 1976).

Immuno-labeling of whole salivary glands, the brain complexes (including prothoracic gland), and imaginal discs from 3rd instar larvae and of brain complexes (including eye disc) from 2 hour pupae were performed as described (Phalle Bde, 2004). Antibodies were diluted as follows: anti-GFP (Fitzgerald Industries Intl.) (1:200), anti-dKeap1 (1:100), anti-CncC (1:100), anti-EcR (Ag10.2, Developmental Studies Hybridoma Bank) (1:200), Alexa Fluor 594 conjugated goat anti-rabbit (Invitrogen) (1:1000). To stain F-actin, pupal brain complexes were incubated in 0.2 U/µl Rhodamine phalloidin (Molecular Probes) in PBST + 1% BSA for 20 minutes. The samples were mounted in VectaShield (Vector Laboratories). For live imaging, tissues were dissected, mounted in PBS and imaged within 5 minutes after dissection. rxYFP signal was visualized using 504 nm excitation and 542 nm emission wavelengths. Rhodamine phalloidin signal was visualized using 540 nm excitation and 565 nm emission wavelengths.

**Immunoblotting**

Four 3rd instar larvae were homogenized in 50 µl ice-cold Buffer (20 mM Tris-HCl pH8.0, 0.2% NP-40, 0.2% Triton X-100, 150 mM NaCl, 5 mM EDTA, 1 mM EGTA, 2 mM $NaVO_3$, protease inhibitor cocktail (Roche) and 1 mM PMSF). The samples were resolved using a NuPAGE 4-12% Bis-Tris gel (Invitrogen). The proteins were transferred to Nitrocellulose membrane (Bio-Rad) and probed using dKeap1 antiserum (1:500), CncC antiserum (1:500) or anti-α-tubulin antibody (12G10, Developmental Studies Hybridoma Bank) (1:500). HRP-conjugated secondary antibodies (GE healthcare UK limited) were used to detect immune complexes.

**Transcript quantitation**

Four 3rd instar larvae or 10 pairs of salivary glands dissected from early wandering 3rd instar larvae in PBS prepared using DEPC water were used for mRNA extraction by the RNeasy kit (Qiagen) following the protocol. Isolated mRNA was treated with RQ1 RNase-Free DNase (Promega) and reverse transcribed using the Transcriptor First Strand cDNA Synthesis Kit (Roche). Real-time qPCR was performed using SYBR Green I Master (Roche) in a LightCycler 480 II (Roche). The relative transcript levels were calculated by assuming that they were proportional to $2^{-Cp}$, and were normalized by the levels of *Rp49* transcripts. Primer sequences were designed using Universal ProbeLibrary software (Roche) and are listed in supplementary material Table S1.

**Statistical analyses**

The significance of the differences in the relative transcript levels measured by RT-qPCR were evaluated using one-way ANOVA.

**Table S1. Primer sequences used to measure the transcript levels by RT-qPCR**

| gene | 5'-primer | 3'-primer |
|---|---|---|
| *Rp49* | CGGATCGATATGCTAAGCTGT | GCGCTTGTTCGATCCGTA |
| *cncC* | GAGGTGGAAATCGGAGATGA | CTGCTTGTAGAGCACCTCAGC |
| *dKeap1* | CAAGGAGTCGGAGATGTCG | GTAGAGGATGCGTGACATGG |
| *Jheh1* | TCACTTCACCACCGATATTCAG | CTTTGTTGTCATCATAAACCATCAG |
| *Jheh2* | TCCTACCCTTCGACATCAGC | GACGACTCAGCTGACCGATT |
| *Jheh3* | ACCTGACCAAGTGGGATGAG | TCGGATACCTTTTCGTGGAT |
| *Cyp6a2* | GCGCAACGAGATCCAAAC | TGTAGAGCCTCAGGGTTTCTG |
| *Cyp6a8* | CAAGATAAGGTTCGGGCTGA | TGGTGTACAGTCGCAGAGTTTC |
| *Cyp12d1* | TGTTTGACTGATGAAATGCAGAT | AGCGAGGTTTGCACAACAAT |
| *gstD1* | TCGCGAGTTTCACAACAGAA | TGAGCAGCTTCTTGTTCAGC |
| *gstD2* | CGGACATTGCCATCCTGT | TGCTGAAGTCGAACTCACTAACTT |
| *gstE1* | GGACTACGAGTACAAGGAGGTGA | TCACATATTCCTCGCTCAGGT |
| *maf-S* | CCGGAGAACCTTAAAGAATCG | TCTCCAGCTCGTCCTTCTGT |
| *Kr-h1* | GAATTCTCCGGACTTTATAGAACAA | GCTGGTTGGCGGAATAGTAA |
| *Jhamt* | TTGACCATGTCACCTCGTTC | TCCGAGAGCTCCTTTCAGAT |

**Supplementary References**


**Brand, A.H., and Perrimon, N.** (1993). Targeted gene expression as a means of altering cell fates and generating dominant phenotypes. *Development* **118**, 401-415.

**Busson, D., and Pret, A.M.** (2007). GAL4/UAS targeted gene expression for studying Drosophila Hedgehog signaling. *Methods Mol Biol* **397**, 161-201.

**Cherbas, L., Hu, X., Zhimulev, I., Belyaeva, E., and Cherbas, P.** (2003). EcR isoforms in Drosophila: testing tissue-specific requirements by targeted blockade and rescue. *Development* **130**, 271-284.

**Johansen, K.M., Cai, W., Deng, H., Bao, X., Zhang, W., Girton, J., and Johansen, J.** (2009). Polytene chromosome squash methods for studying transcription and epigenetic chromatin modification in Drosophila using antibodies. *Methods* **48**, 387-397.

**McGuire, S.E., Mao, Z., and Davis, R.L.** (2004). Spatiotemporal gene expression targeting with the TARGET and gene-switch systems in Drosophila. *Sci STKE 2004*, pl6.

**Mirth, C., Truman, J.W., and Riddiford, L.M.** (2005). The role of the prothoracic gland in determining critical weight for metamorphosis in Drosophila melanogaster. *Curr Biol* **15**, 1796-1807.

**Ostergaard, H., Henriksen, A., Hansen, F.G., and Winther, J.R.** (2001). Shedding light on disulfide bond formation: engineering a redox switch in green fluorescent protein. *EMBO J* **20**, 5853-5862.

**Phalle Bde, S.** (2004). Immunostaining of whole-mount imaginal discs. *Methods Mol Biol* **247**, 373-387.

**Riddiford, L.M., Truman, J.W., Mirth, C.K., and Shen, Y.C.** (2010). A role for juvenile hormone in the prepupal development of Drosophila melanogaster. *Development* **137**, 1117-1126.

**Silver, L.M., and Elgin, S.C.** (1976). A method for determination of the in situ distribution of chromosomal proteins. *Proc Natl Acad Sci U S A* **73**, 423-427.

**Yoshiyama, T., Namiki, T., Mita, K., Kataoka, H., and Niwa, R.** (2006). Neverland is an evolutionally conserved Rieske-domain protein that is essential for ecdysone synthesis and insect growth. *Development* **133**, 2565-2574.